bioRxiv preprint doi: https://doi.org/10.1101/2020.03.25.006569; this version posted March 27, 2020. The copyright holder for this preprint (which was not certified by peer review) is the author/funder. All rights reserved. No reuse allowed without permission.

Analysis of codon usage and evolutionary rates of the 2019-nCoV genes

Maddalena Dilucca[1,2,*], Sergio Forcelloni[1], Athanasia Pavlopoulou[3,4], Alexandros G. Georgakilas[5], Andrea Giansanti[1,6]

1 Physics Department, Sapienza University of Rome, Rome, Italy
2 Liceo Scientifico Statale Augusto Righi, Rome, Italy
3 Izmir Biomedicine and Genome Center (IBG), 35340 Balcova, Izmir, Turkey
4 Izmir International Biomedicine and Genome Institute, Dokuz Eylül University, 35340 Balcova, Izmir, Turkey
5 DNA Damage Laboratory, Physics Department, School of Applied Mathematical and Physical Sciences, National Technical University of Athens (NTUA), Athens, Greece 6 INFN Roma1 unit, Rome, Italy

*** maddalena.dilucca@gmail.com**

Abstract

Severe acute respiratory syndrome coronavirus 2 (2019-nCoV), which first broke out in Wuhan (China) in December of 2019, causes a severe acute respiratory illness with a mortality ranging from 3% to 6%. To better understand the evolution of the newly emerging 2019-nCoV, in this paper, we analyze the codon usage pattern of 2019-nCoV. For this purpose, we compare the codon usage of 2019-nCoV with that of other 30 viruses belonging to the subfamily of orthocoronavirinae. We found that 2019-nCoV shows a rich composition of AT nucleotides that strongly influences its codon usage, which appears to be not optimized to human host. Then, we study the evolutionary pressures influencing the codon usage and evolutionary rates of the sequences of five conserved genes that encode the corresponding proteins (viral replicase, spike, envelope, membrane and nucleocapsid) characteristic of coronaviruses. We found different patterns of both mutational bias and nature selection that affect the codon usage of these genes at different extents. Moreover, we show that the two integral membrane proteins proteins (matrix and envelope) tend to evolve slowly by accumulating nucleotide mutations on their genes. Conversely, genes encoding nucleocapsid (N), viral replicase and spike proteins are important targets for the development of vaccines and antiviral drugs, tend to evolve faster as compared to other ones. Taken together, our results suggest that the higher evolutionary rate observed for these two genes could represent a major barrier in the development of antiviral therapeutics 2019-nCoV.

1 Introduction

The name "coronavirus" is derived from the Greek '*korwna*', that mean crown. The first complete genome of coronavirus (mouse hepatitis virus - MHV), a positive sense, single-stranded RNA virus, was first reported in 1949. It belongs to the family Coronaviridae and ranges from 26.4 (ThCoV HKU12) to 31.7 (SW1) kb in length [10], making it the largest genomes among all known RNA viruses, with G + C contents varying from 32% to 43% [20]. The coronavirinae family consists of four genera based on their genetic properties, including genus:

bioRxiv preprint doi: https://doi.org/10.1101/2020.03.25.006569; this version posted March 27, 2020. The copyright holder for this preprint (which was not certified by peer review) is the author/funder. All rights reserved. No reuse allowed without permission.

Alphacoronavirus, *Betacoronavirus* (subdivided in subgroups A, B, C and D), *Gammacoronavirus* and *Deltacoronavirus*. Coronaviruses can infect humans and many different animal species, including swine, cattle, horses, camels, cats, dogs, rodents, birds, bats, rabbits, ferrets, mink, snake, and other wildlife animals. To date, 30 CoVs genomes have been identified. Only seven CoVs have been identified that infect humans, including Human CoV-229E (HCoV-229E), Human coronavirus NL63 (HCoV-NL63), HumanCoV-OC43 (HCoV-OC43), Human CoV-HKU1 (HCoV-HKU1), Human SARS related coronavirus (SARSr-CoV), Middle East Respiratory Syndrome (MERS-CoV) and SARS CoV 2 (nCoV) [26].

Severe acute respiratory syndrome CoV 2 (2019-nCoV), which first broke out in Wuhan (China) in December of 2019, causes a severe acute respiratory illness with a mortality rate from 3% to 6%. The newly sequenced virus genome encodes two open reading frames (ORFs), ORF1a and ORF1ab, the latter encodes a RNA-dependent RNA polymerase (RdRP) or viral replicase, and four structural proteins [19], [9]: the spike-surface glycoprotein (S), the small envelop protein (E), the matrix protein (M), and the nucleocapsid protein (N).

The phenomenon of codon usage bias exists in many genomes including RNA genomes and it is actually determined by mutation and selection [1]. The choice of synonymous codons is not random for a species, because codon usage varies among species [11] [7]. It is important to study pattern of common codon usage in coronavirus beacuse codon usage bias is one of the most important indicators of a driving force in the evolution of small DNA viruses: for example, mutational bias has been attributed as the major determinant of codon usage variation among RNA viruses [13]. Some studies, in fact, show that the codon usage bias of RNA viruses is low, such as in the Equine infectious anemia virus (EIAV) or Zaire ebolavirus (ZEBOV) [5].

The aim of this study was to carry out a comprehensive analysis of codon usage and composition of coronavirus and explore the possible leading evolutionary determinants of the biases found.

2 Results

2.1 Nucleotide composition

The nucleotide content of 30 coronaviruses coding sequences are calculated. The results reveal that the nucleotide A is the most frequent base and the nucleotide frequencies are in order A >T>G>C [19]. For nCoV we note a different trend T>A>G>C, but in totally AT% is more used than GC% (See Table 3). The GC content in nCoV is 0.373 ± 0.05.

2.2 All the sequenced 2019-nCoV genomes share a common codon usage

We downloaded the protein-coding sequences of 2019-nCoV from GIDAID database, by classifying each n-CoV based on the geographic location where they are sequenced (see tree in A2). For each n-CoV genome, we calculated the relative synonymous codon usage (RSCU), in the form of a 61-component vector. In Fig A1, we show the heatmap and the associated clustering of these vectors. Despite the high mutation rate that characterizes 2019-nCoV genome [30], [4], the overall codon usage bias among 2019-nCoV strains appears to be similar. Moreover, their associated vectors did not cluster according to geographic location, thus confirming the common origin of these genomes. Therefore, we will consider a unique vector to represent 2019-nCoV in the following analyses.

bioRxiv preprint doi: https://doi.org/10.1101/2020.03.25.006569; this version posted March 27, 2020. The copyright holder for this preprint (which was not certified by peer review) is the author/funder. All rights reserved. No reuse allowed without permission.

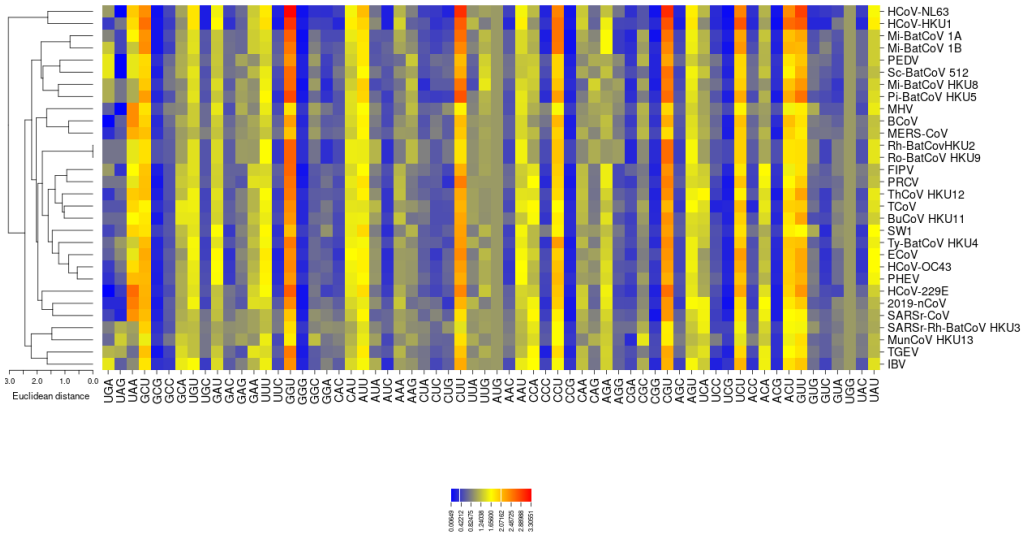

Figure 1. Clustering of the RSCU vectors associated to coronavirus. Analysis of codon bias in coronavirus genomes reveal that the newly identified coronavirus 2019-nCoV Wuhan-Hu-1 sequence was closer to SARSr-CoV as in the reconstructed phylogenetic tree shown in Figure A3. Heatmap are drawn with the CIMminer software [25], which uses Euclidean distances and the average linkage algorithm.

2.3 Codon usage of 2019-nCoV genome strains

We compared the codon usage of 2019-nCoV with that of the other coronavirus genomes. For this purpose, we used the RSCU which is a biologically relevant metric of distance between the codon usage in the protein-coding sequences of these genomes. In Fig. 1, we report the heatmap of the RSCU values associated with the coronavirus. The RSCU values of the majority of the codons scored between 0 and 3.1 (see legend in Figure 1). Interestingly, analysis of codon bias in coronavirus genomes reveal that the newly identified coronavirus 2019-nCoV Wuhan-Hu-1 sequence has a clear origin from other beta-CoV's and is closer, specifically, to SARSr-CoV, consistent with their phylogenetic relationships (Figure A3). In line with previous observations, we show that the mean CpG relative abundance in the coronavirus genomes is markedly suppressed [27]. Specifically, GGG, GGC, CCG (pyrimidine-CpG) and ACG (purine-CpG) present a very low frequence of occurrence, probably due to the relative tRNA abundance of the host. In fact, in human the abundance of tRNA in codons GGG, GGC, CCG and ACG are respectavely: 0, 0, 4 and 7.

In 2019-nCoV, the most frequently used codons are CGU (arginine, 2.34 times) and GGU (glycine, 2.42), whereas the least used codons are GGG (glycine) and UCG (serine). We also note the most frequently used codons for each amino acid, ended in either U or A. [5]

2.4 The codon usage of 2019-nCoV is not optimized to the host.

To measure the codon usage bias in the coronavirus genomes, we used the effective number of codons (ENC) value and the Competition Adaptation Index (CAI). In Table 2 and 3, we report the ENC and CAI values for all the coronaviruses we considered in this work. To visually enhance the differences among the codon

bioRxiv preprint doi: https://doi.org/10.1101/2020.03.25.006569; this version posted March 27, 2020. The copyright holder for this preprint (which was not certified by peer review) is the author/funder. All rights reserved. No reuse allowed without permission.

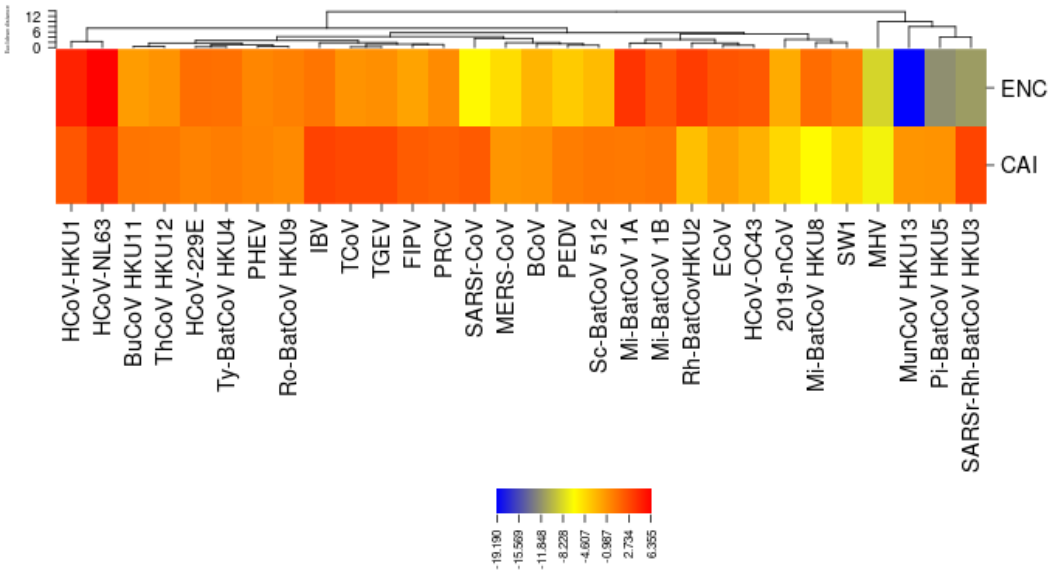

Figure 2. Z-score values. Z-score is calculated for two codon bias indexes ENC and CAI. We show in figure that a lot of coronavirus have a codon usage major tha the average value of the family (Z-score 3). For what concerns 2019-nCoV, it presents average CAI and ENC higher than the average too.

usage of these coronaviruses we calculated Zscore of a single virus in relation to the other members of the CoV subfamily. Interestingly, the ENC value associated to 2019-nCoV (51.9 ± 2.59) is lower than the average of all Coronaviruses, meaning that 2019-nCoV uses a broader set of synonymous codons in its coding sequences. We also note that CAI of 2019-nCoV (0.727 ± 0.054) is lower than the average one, underscoring that this coronavirus tend to use codons that are not optimized to the host. We calculate similarity index (SiD) to measure the effect of codon usage bias of the host (human) on the 2019-nCoV genes. The SiD values range from 0 to 1, with higher values indicating that the host has a dominant effect on the usage codons. [16] In our case SiD for 2019-nCoV is equal to 0.78.

2.5 Genes

The genome of the newly emerging 2019-nCoV consists of a single, positive-stranded RNA, that is approximately 30K nucleotides long. The overall genome is organizated similar to other coronaviruses. Ceraolo et al. performed a cross-species analysis for all proteins encoded by the 2019-nCoV (see Figure 3-4 in [3]). The newly sequenced virus genome encodes polyproteins, common to all betacoronavirus, which are further cleaved into the individual structural proteins E, M, N and S, as well the non-structural RdRP [28]. So, only five virall genes are classified according to their viral location and studied for each virus because the short length and insufficient codon usage diversity of the other genes might have biased the results. The corresponding gene products including S protein regulates virus attachment to the receptor of the target host cell [2]; the E protein functions to assemble the virions and acts as an ion channel [18], the M protein plays a role in virus assembly and is involved in biosynthesis of new virus particles [17] the N protein forms the ribonucleoprotein complex with the virus RNA [19]. Finally, RdRP catalyzes viral RNA syntesis. We calculate for these five proteins the RSCU vectors in each virus of the dataset (see Figure 3). We show that only for gene E, M and N 2019-nCoV cluster with SARSr-CoV and SARSr-Rh-BatCoV HKU3,

bioRxiv preprint doi: https://doi.org/10.1101/2020.03.25.006569; this version posted March 27, 2020. The copyright holder for this preprint (which was not certified by peer review) is the author/funder. All rights reserved. No reuse allowed without permission.

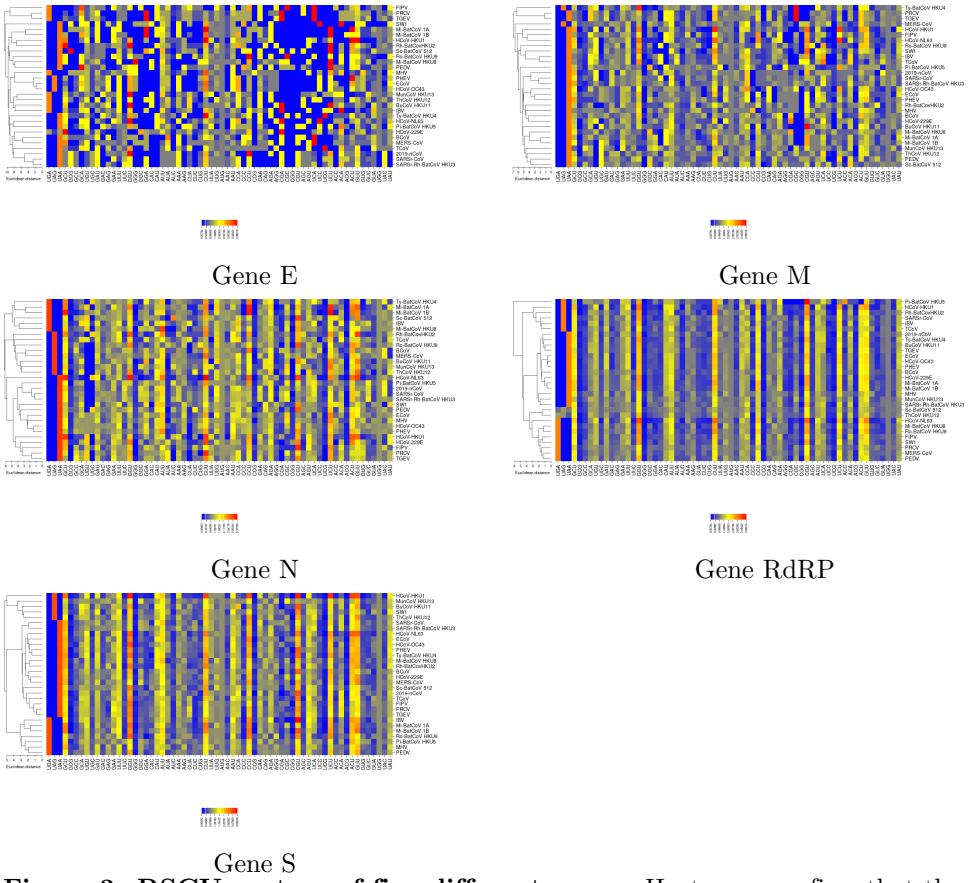

Figure 3. RSCU vectors of five different genes. Heatmaps confirm that the newly identified coronavirus 2019-nCoV Wuhan-Hu-1 sequence is closer to SARS and HCoV 229E, except for gene RdRP and gene S.

consistent with the inferred phylogeny shown in Figure A3.

2.6 The ENC plot analysis of individual genes of 2019-nCoV

To further investigate which factors account for the low codon usage bias of the different genes in coronavirus, we analyzed the relationship between the ENC value and the percentage of G or C in the third positioncodons (GC3s). In Figure 4, we show separately the ENC-plots obtained for the five genes (M, N, S, E, and RdRP), together with the Wright's theoretical curve, corresponding to the case when the codon usage is only determined by the GC3s [29]. We would like to point out that if mutational bias, as quantified by GC-content in the generally neutral 3rd codon position, is the main factor in determining the codon usage among these genes, the corresponding point in the ENC-plot should lie on or just below Wright's curve. In Figure 4, all distributions lie below the theoretical curve, an indication that not only mutational bias but also natural selection plays a non-negligible role in the codon choice in all genes. This is exemplified by the violinplots in Figure 5 of the distances between the genes and Wright's theoretical curve. Genes N, S, and RdRP are more scattered below the theoretical curve than those of genes M and E, implying that in the latter the codon usage patterns are pretty consistent with the effects of mutational bias. Interestingly, data points corresponding to the gene N, which is the major viral structural component needed to protect and encapsidate

bioRxiv preprint doi: https://doi.org/10.1101/2020.03.25.006569; this version posted March 27, 2020. The copyright holder for this preprint (which was not certified by peer review) is the author/funder. All rights reserved. No reuse allowed without permission.

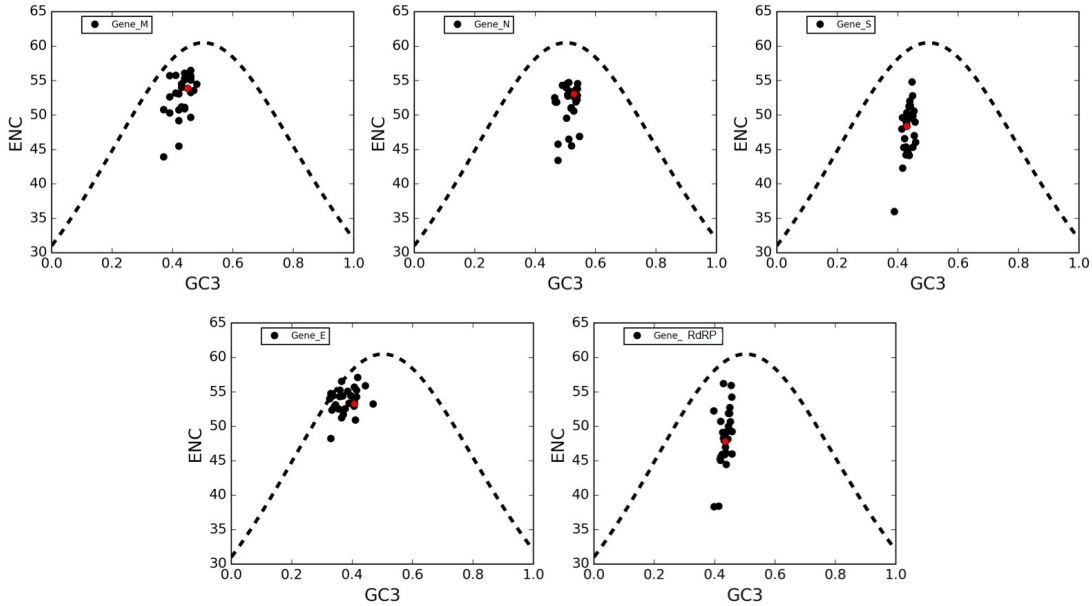

Figure 4. ENC-plots of genes M, N, S, E, RdRP. In these plots, each point corresponds to a single gene. The black-dotted lines in all panels are plots of Wright's theoretical curve corresponding to the case of a CUB merely due to mutational bias (no selective pressure). Red dots represent 2019-nCoV genes.

the viral RNA, is localized around GC3=0.5 (See Figure 4). This means that the displacement under the curve most likely reflects the selective pressure exerted on this gene. Conservely, all other genes show a displacement towards lower values of GC3-content, thus corroborating our previously mentioned observation that coronaviruses tend to use codons that end with A and U (see section 2.3).

2.7 Neutrality plot

A neutrality plot analysis was performed to estimate the role of mutational bias and natural selection in shaping the codon usage patterns of the five genes under investigation. In this plot, the average GC-content in the first and second positions of codons (GC12) is plotted against GC3s, which is considered as a pure mutational parameter. In Figure 5, we report the neutrality plots obtained for genes M, N, S, E, RdRP, together with the best-fit lines and the slopes associated with them.

The rationale to understand the results is that the wider is the deviation between the slope of the regression line and the bisector, the stronger is the action of selective pressure. All correlation are highly significant (Spearman correlation - R^2 analysis, p-value¡0.0001). By comparing the divergences between the regression lines and the bisectors in each panel, we reveal that the five genes here considered are subject to different balance between natural selection and mutational bias. Specifically, in line with the ENC-plot analyses, the genes S and RdRP present the largest deviations of their regression lines from the bisector lines and, therefore, a stronger action of natural selection. Conversely, the regression line for the gene M is closer to the bisector than the other genes, meaning that the this gene is the least one subject to the action of natural selection. Finally, the genes E and N are intermediate between the previous cases.

It is worth noting that almost all data points are located below the bisector lines, implying a selective tendency for a higher AT content in the first two codon positions than in the third one. In addition, both GC3 and GC12 are lower than

bioRxiv preprint doi: https://doi.org/10.1101/2020.03.25.006569; this version posted March 27, 2020. The copyright holder for this preprint (which was not certified by peer review) is the author/funder. All rights reserved. No reuse allowed without permission.

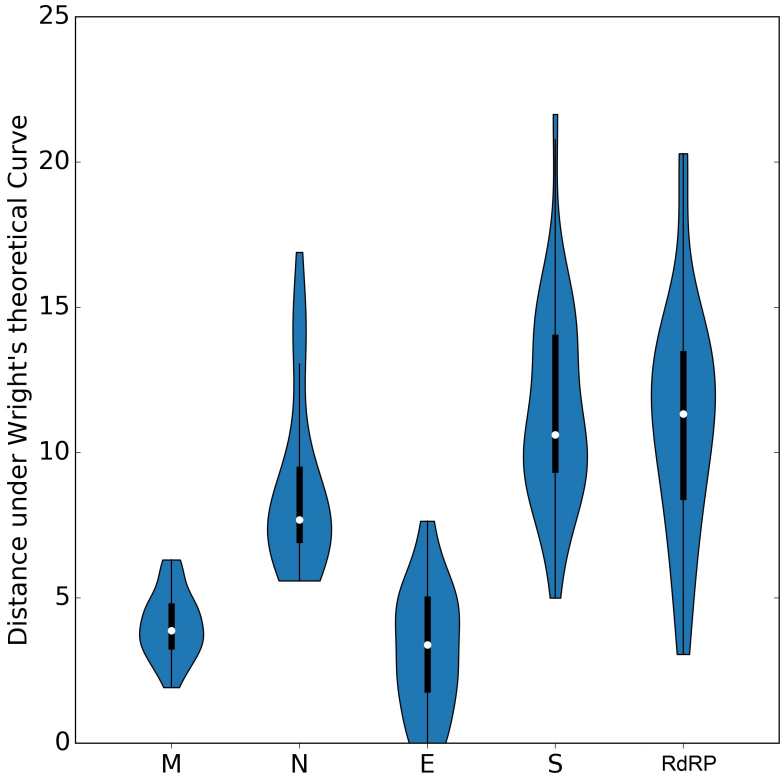

Figure 5. Distances from Wright's curve. Box plots are calculated for each gene for values of distance from theoretical Wright's curve. Genes N, S, and ORF1ab are more scattered below the theoretical curve than those of genes M and E, implying that in the latter the codon usage patterns are pretty consistent with the effects of mutational bias.

bioRxiv preprint doi: https://doi.org/10.1101/2020.03.25.006569; this version posted March 27, 2020. The copyright holder for this preprint (which was not certified by peer review) is the author/funder. All rights reserved. No reuse allowed without permission.

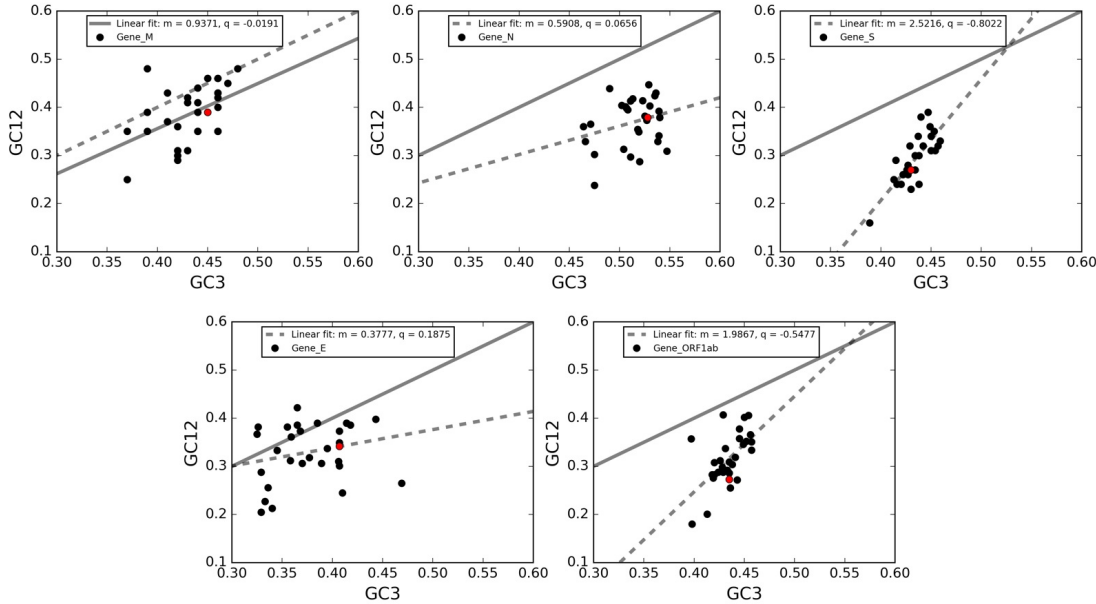

Figure 6. Neutrality plot of genes M, N, S, E, RdRP. In these plots, each point corresponds to a single gene in a virus. The solid black lines in all panels are the bisectors corresponding to the case of a CUB merely due to mutational bias (no selective pressure). The black-dotted lines are the linear regressions. Red dots represent 2019-nCoV genes.

0.5, thus showing a general preference for A and T bases in all three codon positions. Interestingly, data points associated to gene M and E are closer to the bisector lines as compared to gene N, S, and RdRP. This observation means that the GC content in the first two codon positions tend to be in proportion to GC3 in gene M and E, and this partially explains the closeness of these two genes to the Wright theoretical curve in Figure 4.

2.8 Forsdyke plot

We analyze the rate of evolution that characterize these genes by confronting the nucleotide sequences of the newly emerging 2019-nCoV and their corrisponding protein sequences with those of other coronaviruses here considered. Each gene of 2019-nCoV was compared to the orthologous gene in one of the 30 coronaviruses to estimate evolutionary divergences. Each pair of homologous genes is represented by a point in the Forsdyke plot [8], which correlates protein divergence with DNA divergence. Each point in Forsdyke plots measures the divergence between pairs of orthologous genes in the two species, as projected along with the phenotypic (protein) and nucleotidic (DNA) axis. Thus, the slope is an estimation of the fraction of DNA mutations that result in amino acid substitutions in the speciation process between two species [8]. In Figure 7, we show separately for each gene the associated Forsdyke plot.

Overall, protein and DNA sequence divergences are linearly correlated, and these correlations can be expressed through slopes and intercepts of the regression lines.

Overall, protein and DNA sequence divergences are linearly correlated, and these correlations can be expressed through slopes and intercepts of the regression lines.

Genes M and E show quite low slopes, indicating that these proteins tend to

bioRxiv preprint doi: https://doi.org/10.1101/2020.03.25.006569; this version posted March 27, 2020. The copyright holder for this preprint (which was not certified by peer review) is the author/funder. All rights reserved. No reuse allowed without permission.

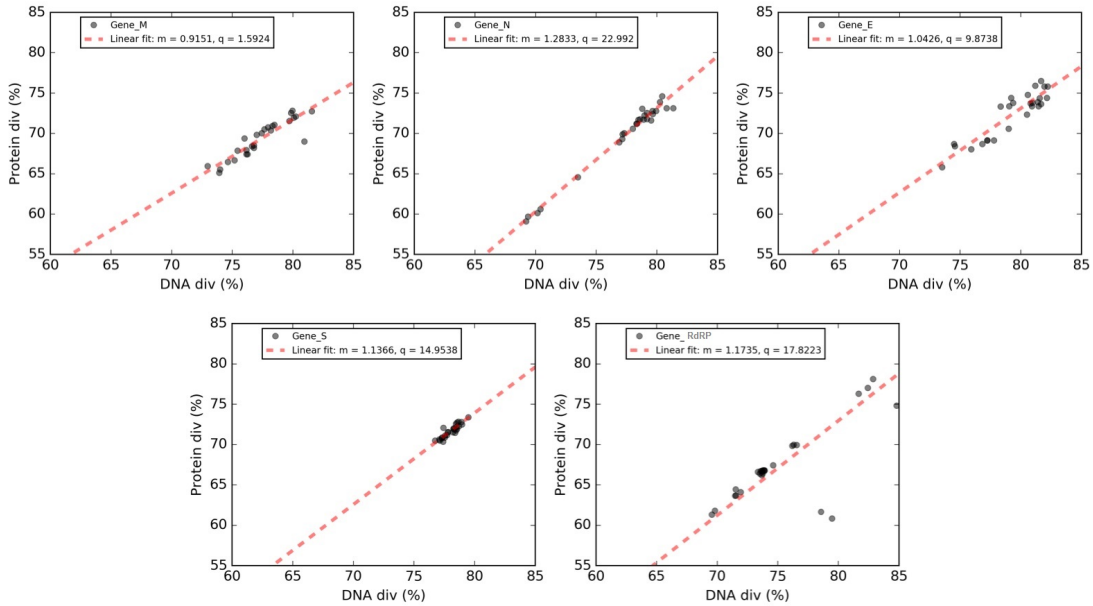

Figure 7. Forskdyke plots of genes M, N, S, E, RdRP. Phenotype (Protein div) vs. nucleotide (DNA div) sequence divergence between 2019-nCoV and homologous genes in the other coronaviruses. Each point corresponds to an individual gene. In each panel, we report the best-fit line in red, together with the associated values of the slope (m) and the intercept (q) in the legend.

evolve slowly by accumulating nucleotide mutations on their genes. Conversely, the steeper slopes for genes N, RdRP, and S indicate that these genes tend to evolve faster compared to other ones. A plausible explanation for this observation is that protein N due to its immunogenicity, has been frequently used to generate specific antibodies against various animal coronavirus, including in SARS [24]. The viral replicase polyprotein that is essential for the replication of viral RNA and, finally, the gene S encodes the protein that is responsible for the "spikes" present on the surface of coronaviruses. Taken together, our results suggest that the higher evolutionary rate observed for these proteins could represent a major obstacle to in the development of a antiviral therapeutics against 2019-nCoV.

2.9 Tables

3 Discussion

To investigate the factors leading to the 2019-nCoV and other viruses related to codon usage patterns, several analytical methods were used in our study. First, the RSCU value of the 2019-nCoV was calculated. Despite the high mutation rate that characterize 2019-nCoV, we do not show differences in codon usage between these genomes.Moreover, their associated vectors did not cluster for geographically positon, thus confirming the common origin of these genomes. The nucleotide composition confirm higher AT% content and low GC% content as it is common in RNA viruses such as Severe Acute Respiratory Syndrome (SARS) [**?**]. The results indicate also that codon usage bias exists and that the 2019-nCoV preferred codons almost all end in U. The codon usage bias was further confirmed by the mean ENC value of 51.9 (a value greater than 45 is considered as a slight codon usage bias due to mutation pressure or nucleotide compositional constraints). The same analysis is effectuated with CAI index, that it is calculated on the with RNA

bioRxiv preprint doi: https://doi.org/10.1101/2020.03.25.006569; this version posted March 27, 2020. The copyright holder for this preprint (which was not certified by peer review) is the author/funder. All rights reserved. No reuse allowed without permission.

Table 1. Coronaviruses (CoVs) in dataset. We report family (a for alphacoronavirus, b for betacoronavirus, c for gammacoronavirus, d for deltacoronavirus), name, abbreviation and NCBI code.

a	Feline infectious peritonitis virus	FIPV	NC_002306.3
a	Human coronavirus 229E	HCoV-229E	NC_002645.1
a	Human coronavirus NL63	HCoV-NL63	NC_005831.2
a	Miniopterus bat coronavirus 1A	Mi-BatCoV 1A	NC_010437.1
a	Miniopterus bat coronavirus 1B	Mi-BatCoV 1B	EU420137.1
a	Miniopterus bat coronavirus HKU8	Mi-BatCoV HKU8	NC_010438.1
a	Porcine epidemic diarrhea virus	PEDV	NC_003436.1
a	Porcine respiratory coronavirus	PRCV	DQ811787.1
a	Rhinolophus bat coronavirus HKU2	Rh-BatCovHKU2	NC_009988.1
a	Scotophilus bat coronavirus 512	Sc-BatCoV 512	NC_009657.1
a	Transmissible gastroenteritis virus	TGEV	NC_038861.1
b	Bovine coronavirus	BCoV	NC_003045.1
b	Equine coronavirus	ECoV	LC061274.1
b	Human coronavirus HKU1	HCoV-HKU1	NC_006577.2
b	Human coronavirus OC43	HCoV-OC43	NC_006213.1
b	Mouse hepatitis virus	MHV	NC_001846.1
b	Porcine hemagglutinating encephalomyelitis virus	PHEV	DQ011855.1
b	**Severe acute respiratory syndrome-related coronavirus 2**	**2019-nCoV**	NC_045512.2
b	Severe acute respiratory syndrome-related coronavirus	SARSr-CoV	NC_004718.3
b	SARS-related Rhinolophus bat coronavirus HKU3/	SARSr-Rh-BatCoV HKU3	NC_009694.1
b	Middle East respiratory syndrome-related coronavirus	MERS-CoV	NC_019843.3
b	Bat coronavirus HKU9-1	Ro-BatCoV HKU9	NC_009021.1
b	Pipistrellus bat coronavirus HKU5	Pi-BatCoV HKU5	NC_009020.1
b	Tylonycteris bat coronavirus HKU4	Ty-BatCoV HKU4	NC_009019.1
c	Avian infectious bronchitis virus	IBV	NC_001451.1
c	Beluga whale coronavirus SW1	SW1	NC_010646.1
c	Turkey coronavirus	TCoV	NC_010800.1
d	Bulbul coronavirus HKU11-934	BuCoV HKU11	NC_011547.1
d	Munia coronavirus HKU13-3514	MunCoV HKU13	NC_011550.1
d	Thrush coronavirus HKU12-600	ThCoV HKU12	NC_011549.1

of codons expressed most often. This suggests that the RNA viruses with high ENC values (and low CAI) adapt to the host with various preferred codons. So a low biased codon usage pattern might allow the virus make use of several codons for each amino acid, and might be beneficial for viral replication and translation in the host cells. The The ENC-plot analysis reveals that natural selection plays an important role in the codon choice of the five conserved viral genes here considered: RdRP, S, E, M, and N. However, genes N, S, and ORF1ab are more scattered below the theoretical curve than those of genes M and E, implying that in the latters the codon usage is under more strict control by mutational bias. According with this analysis, the genes S and RdRP present the largest deviations of their linear regressions from the bisectors lines in the neutrality plot analysis that implies a stronger action of natural selection. Conversely, the regression line for the gene M is closer to the bisector than the other genes, meaning that this

bioRxiv preprint doi: https://doi.org/10.1101/2020.03.25.006569; this version posted March 27, 2020. The copyright holder for this preprint (which was not certified by peer review) is the author/funder. All rights reserved. No reuse allowed without permission.

Table 2. Codon usage bias of different coronaviruses.

Abbr.	ENC	CAI
BCoV	52.089± 2.357	0.690 ± 0.040
BuCoV HKU11	51.414 ± 1.855	0.679 ± 0.045
ECoV	49.311 ± 4.024	0.691 ± 0.025
FIPV	51.568 ± 1.999	0.667 ± 0.048
HCoV-HKU1	44.582 ± 7.331	0.675 ± 0.021
HCoV-229E	50.290 ± 3.629	0.684 ± 0.023
HCoV-NL63	44.675± 5.350	0.664 ± 0.028
HCoV-OC43	49.573 ± 3.660	0.692 ± 0.020
IBV	50.654 ± 2.900	0.653 ± 0.053
MERS-CoV	53.087 ± 2.526	0.689± 0.029
MHV	53.628 ± 1.725	0.712 ± 0.023
Mi-BatCoV 1A	48.233± 3.810	0.682 ± 0.028
Mi-BatCoV 1B	49.311 ± 4.116	0.681± 0.026
Mi-BatCoV HKU8	50.120 ± 4.139	0.702 ± 0.016
MunCoV HKU13	53.963 ± 0.863	0.691± 0.041
2019-nCoV	51.984 ± 2.596	0.727 ± 0.054
PEDV	52.442 ± 2.153	0.683± 0.037
PHEV	51.093± 3.553	0.684 ± 0.024
Pi-BatCoV HKU5	53.913 ± 1.359	0.691 ± 0.042
PRCV	51.276 ± 3.154	0.675 ± 0.029
Rh-BatCovHKU2	48.084 ± 4.491	0.693 ± 0.016
Ro-BatCoV HKU9	50.910 ± 2.311	0.686 ± 0.033
SARSr-CoV	53.642 ± 2.436	0.670± 0.038
SARSr-Rh-BatCoV HKU3	54.305± 1.613	0.667 ± 0.030
Sc-BatCoV 512	52.379 ± 2.631	0.680 ± 0.043
SW1	50.865± 1.791	0.706 ± 0.027
TCoV	51.343 ± 2.317	0.659 ± 0.046
TGEV	51.393 ± 3.269	0.665 ± 0.037
ThCoV HKU12	51.432 ± 2.833	0.681 ± 0.031
Ty-BatCoV HKU4	50.374 ± 3.742	0.683 ± 0.032

Table 3. Statistics in 2019-nCoV.

	A	C	G	T
ObsN	8708	5338	5720	9369
Freq.	0.298	0.183	0.196	0.321

bioRxiv preprint doi: https://doi.org/10.1101/2020.03.25.006569; this version posted March 27, 2020. The copyright holder for this preprint (which was not certified by peer review) is the author/funder. All rights reserved. No reuse allowed without permission.

gene is the least one subject to the action of natural selection. Finally, the genes E and N are intermidiate between the previous cases.

To analyze the rate of evolution that characterize these genes by confronting the nucleotide sequences we use the Forsdyke plot thar correlates protein divergence with DNA divergence. The two proteins M and E show quite low slopes, indicating that these proteins tend to evolve slowly by accumulating nucleotide mutations on their genes. Conversely, the steeper slopes for gene N and RdRP and the gene S encoding for the S protein, which is responsible for the "spikes" present on the surface of coronaviruses, indicate that these three genes, and therefore their corresponding protein products, tend to evolve faster compared to the other two genes. Findings of the present study could be directed to be useful for developing diagnostic reagents and probes for detecting a range of viruses and isolates in one test and for vaccine development, using the information about codon usage patterns in these genes.

4 Materials and Methods

4.1 Sequence data analyzed

The complete coding genomic sequences of 306 isolates of nCov reported across the world to date, were obtained from GISAID (available at $https://www.gisaid.org/epiflu-applications/next-hcov-19-app/$) and NCBI viruses database accessed as on 17 March 2020.

Then the sequences are selected according to their geographical distribution, the isolation date, and the host species. The complete coding genomic sequences of 30 coronaviruses were downloaded from the National Center for Biotechnological Information (NCBI) (available at $https://www.ncbi.nlm.nih.gov/$). For each virus we consider in following alphabetical order genes: E, M, N, RdRP and S.

4.2 Nucleotide Composition Analysis

The diverse nucleotide compositional properties are calculated for the coding sequences of 30 CoV genomes. These compositional properties comprise the frequencies of occurrence of each nucleotide (A, T, G, and C), AU and GC contents, nucleotides G + C at the first (GC1), second (GC2), and third codon positions (GC3). To calculate these values we use an in-house Python script. We calculate, also, mean frequencies of nucleotides G + C at the first and the second positions (GC12).

4.3 RSCU

$RSCU$ vectors for all the genomes were computed by using an in-house Python script, following the formula:

$$RSCU_i = \frac{X_i}{\frac{1}{N_i}\sum_{j=1}^{n_i} X_j} \tag{1}$$

In the $RSCU_i$ X_i is the number of occurrences, in a given genome, of codon i, and the sum in the denominator runs over its n_i synonymous codons. If the $RSCU$ value for a codon i is equal to 1, this codon was chosen equally and randomly. Codons with $RSCU$ values greater than 1 have positive codon usage bias, while those with value less than 1 have relatively negative codon usage bias [**?**]. $RSCU$ heat maps were drawn with the CIMminer software [25], which uses Euclidean distances and the average linkage algorithm.

bioRxiv preprint doi: https://doi.org/10.1101/2020.03.25.006569; this version posted March 27, 2020. The copyright holder for this preprint (which was not certified by peer review) is the author/funder. All rights reserved. No reuse allowed without permission.

4.4 Effective Number of Codons Analysis

ENC is an estimate of the frequency of different codons used in a coding sequence. In general, ENC ranges from 20 (when each aminoacid is coded by just one and the same codon) to 61 (when all synonymous codons are used on an equal footing). Given a sequence of interest, the computation of ENC starts from F_α, a quantity defined for each family α of synonymous codons (one for each amino acid):

$$F_\alpha = \left(\frac{n_{k\alpha}}{n_\alpha}\right)^2 \tag{2}$$

where m_α is the number of different codons in α (each one appearing $n_{1_\alpha}, n_{2_\alpha}, ..., n_{m_\alpha}$ times in the sequence) and $n_\alpha = \sum_{k=1}^{m_\alpha} n_{k_\alpha}$.

ENC then weights these quantities on a sequence:

$$ENC = N_s + \frac{K_2 \sum_{\alpha=1}^{K_2} n_\alpha}{\sum_{\alpha=1}^{K_2}(n_\alpha F_\alpha)} + \frac{K_3 \sum_{\alpha=1}^{K_3} n_\alpha}{\sum_{\alpha=1}^{K_3}(n_\alpha F_\alpha)} + \frac{K_4 \sum_{\alpha=1}^{K_4} n_\alpha}{\sum_{\alpha=1}^{K_4}(n_\alpha F_\alpha)} \tag{3}$$

where N_S is the number of families with one codon only and K_m is the number of families with degeneracy m (the set of 6 synonymous codons for Leu can be split into one family with degeneracy 2, similar to that of Phe, and one family with degeneracy 4, similar to that, e.g., of Pro).

We have evaluated ENC by using the implementation in $DAMBE$ 5.0 [31].

4.5 Codon Adaptation Index

Codon adaptation index CAI [**?**] is used to quantify the codon usage similarities between the virus and host coding sequences. The principle behind CAI is that codon usage in highly expressed genes can reveal the optimal (*i.e.*, most efficient for translation) codons for each amino acid. Hence, CAI is calculated based on a reference set of highly expressed genes to assess, for each codon i, the relative synonymous codon usages ($RSCU_i$) and the relative codon adaptiveness (w_i):

$$RSCU_i = \frac{X_i}{\frac{1}{n_i}\sum_{j=1}^{n_i} X_j}; \qquad w_i = \frac{RSCU_i}{\max_{j=1,\ldots,n_i}\{RSCU_j\}}; \tag{4}$$

In the $RSCU_i$, X_i is the number of occurrences of codon i in the genome, and the sum in the denominator runs over the n_i synonyms of i; $RSCU$s thus measure codon usage bias within a family of synonymous codons. w_i is then defined as the usage frequency of codon i compared to that of the optimal codon for the same amino acid encoded by i—*i.e.*, the one which is mostly used in a reference set of highly expressed genes. The CAI for a given gene g is calculated as the geometric mean of the usage frequencies of codons in that gene, normalized to the maximum CAI value possible for a gene with the same amino acid composition:

$$CAI_g = \left(\prod_{i=1}^{l_g} w_i\right)^{1/l_g}, \tag{5}$$

where the product runs over the l_g codons belonging to that gene (except the stop codon).

This index values range from 0 to 1, where the score 1 represents the tendency of a gene to always use the most frequently used synonymous codons in the host. The CAI analysis of these coding sequences are performed using $DAMBE$ 5.0 [31]. The synonymous codon usage data of different hostes (human- Homo sapiens and other species) are retrieved from the codon usage database (available at: http://www.kazusa.or.jp/codon/).

bioRxiv preprint doi: https://doi.org/10.1101/2020.03.25.006569; this version posted March 27, 2020. The copyright holder for this preprint (which was not certified by peer review) is the author/funder. All rights reserved. No reuse allowed without permission.

To study the patterns of codon bias in the coronaviruses, we use Z-score values:

$$Z_v[(ENC)] = \frac{\langle ENC \rangle_{family} - \langle ENC \rangle_v}{\sigma_v / \sqrt{N_v}}, \tag{6}$$

where $\langle ENC \rangle_{family}$ is the average of the ratio within a codon bias index in a family of a virus v, $\langle ENC \rangle_v$ and σ_v are the average value of ENC and its standard deviation over the whole virus v, and N_v is the number of virus in the family (we use the standard deviation of the mean as we are comparing average values).

The same Z-score is evalueted for codon bias index CAI.

4.6 ENC plot

ENC-plot analysis was performed to estimate the relative contributions of mutational bias and natural selection in shaping CUB of genes encoding for proteins that are crucial for 2019-nCoV: RdRP, the spike-surface glycoprotein (protein S), the small envelop protein (protein E), the matrix protein (M), and the nucleocapsid protein (N). The ENC-plot is a plot in which the ENC is the ordinate and the GC3 is the abscissa. Depending on the action of mutational bias and natural selection, different cases are discernable. If a gene is not subject to selection, a clear relationship is expected between ENC and GC3 [**?**]:

$$ENC = 2 + s + \frac{29}{s^2 + (1-s)^2} \tag{7}$$

where s represents the value of GC_3 [**?**]. Genes for which the codon choice is only constrained by mutational bias are expected to lie on or just below the Wright's theoretical curve. Alternatively, if a particular gene is subject to selection, it will fall below Wright's theoretical curve. In this case, the vertical distance between the point and the theoretical curve provides an estimation of the relative extent to which natural selection and mutational bias affect CUB.

To evaluate scatter of dots from theoretical Wright's curve, we calculate the module of distance and we drawn box plot calculated with an in-house Python script.

4.7 Neutrality plot

We used a neutrality plot analysis [**?**] to estimate the relative contribution of natural selection and mutational bias in shaping CUB of five crucial genes in the research field aiming to develop a vacine against 2019-nCoV: M, N, S, RdRP, and E. In this analysis, the GC1 or GC2 values (ordinate) are plotted against the GC3 values (abscissa), and each gene is represented as a single point on this plane. In this case, the three stop codons (TAA, TAG, or TGA) and the three codons for isoleucine (ATT, ATC, and ATA) were excluded in calculation of GC3, and two single codons for methionine (ATG) and tryptophan (TGG) were excluded in all three (GC1, GC2, GC3) (Sueoka 1988). For each gene, we separately performed a Spearman correlation analysis between GC1 and GC2 with the GC3. If the correlation between GC1/2 and GC3 is statistically significant, the slope of the regression line provides a measure of the relative extent to which natural selection and mutational bias affect CUB of these genes (Sueoka 1999). In particular, if the mutational bias is the driving force that shapes CUB, then the corresponding data points should be distributed along the bisector (slope of unity). On the other hand, if natural selection also affects the codon choice of a family of genes, then the corresponding regression line should diverge from the bisector. Thus, the extent of the divergence between the regression line and the bisector indicates that the extent of codon choice due to the natural selection.

bioRxiv preprint doi: https://doi.org/10.1101/2020.03.25.006569; this version posted March 27, 2020. The copyright holder for this preprint (which was not certified by peer review) is the author/funder. All rights reserved. No reuse allowed without permission.

4.8 Forsdyke plot

To study the evolutionary rates of genes M, N, S, RdRP, and E, we performed an analysis by using our previously defined Forsdyke plot [8]. Each gene in 2019-nCoV (taken as a reference) was confronted with the homologous gene in one of the 30 coronaviruses considered in this analysis. Each pair of homologous genes is represented by a point in the Forsdyke plot, which correlates protein divergence with DNA divergence (see Methods in [8] for details). The protein sequences were aligned using Biopython. The DNA sequences were then aligned using the protein alignments as templates. Then, DNA divergences and protein divergences were assessed as axplained in Methods in [8] by counting the number of mismatches in each pair of aligned sequences. Thus, each point in Forsdyke plots measures the divergence between pairs of homologous genes in the two species, as projected along with the phenotypic (protein) and nucleotidic (DNA) axis.The first step in each comparison is to compute the regression line between protein vs. DNA sequence divergence in the Forsdyke plot getting values of intercept and slope for each variant of gene. To test whether the regression parameters associated with each variant are different or not, we have followed a protocol founded by F-statistic test, considering a p-value ≤ 0.05.

4.9 Phylogenetic analysis

To explore the evolutionary relationships among the four genera of coronaviruses, phylogenetic analysis of the full-length genomic sequences of the 30 CoVs listed in Table 1 was performed. The sequences were aligned with the usage of ClustalO [21], [22]. The resulting multiple sequence alignment was used to build a phylogenetic tree by employing a maximum-likelihood (ML) method implemented in the software package MEGA version 10. 1 [15]. ModelTest-NG [6] was used to select the best-fit evolutionary model of nucleotide substitution, that is, GTR + G + I. Bootstrap analysis (100 pseudo-replicates) was conducted in order to evaluate the statistical significance of the inferred trees.

A

A.1

References

1. Belalov IS, Lukashev AN, Causes and Implications of Codon Usage Bias in RNA Viruses PLoS One. 2013; 8(2): e56642. Published online 2013, Feb 25. doi: 10.1371/journal.pone.0056642
2. Cavanagh D.The Coronavirus Surface Glycoprotein, the Coronaviridae Springer (1995), pp. 73-113
3. Ceraolo C., Giorgi FM. Genomic variance of the 2019-nCoV coronavirus, DOI: 10.1002/jmv.25700
4. Cao Y, Li L, Feng Z. et al. Comparative genetic analysis of the novel coronavirus (2019-nCoV/SARS-CoV-2) receptor ACE2 in different populations. Cell Discov 6, 11 (2020). https://doi.org/10.1038/s41421-020-0147-1
5. Chen Y, Xu Q, Yuan X, Li X. Analysis of the codon usage pattern in Middle East Respiratory Syndrome Coronavirus, Oncotarget, 2017, Vol. 8, (No. 66), pp: 110337-110349
6. Darriba D,, Posada D, Kozlov AM, Stamatakis A,, Morel B, Flouri T. ModelTest-NG: A New and Scalable Tool for the Selection of DNA and Protein Evolutionary Models., Mol Biol Evol. 2020 Jan 1;37(1):291-294. doi: 10.1093/molbev/msz189

bioRxiv preprint doi: https://doi.org/10.1101/2020.03.25.006569; this version posted March 27, 2020. The copyright holder for this preprint (which was not certified by peer review) is the author/funder. All rights reserved. No reuse allowed without permission.

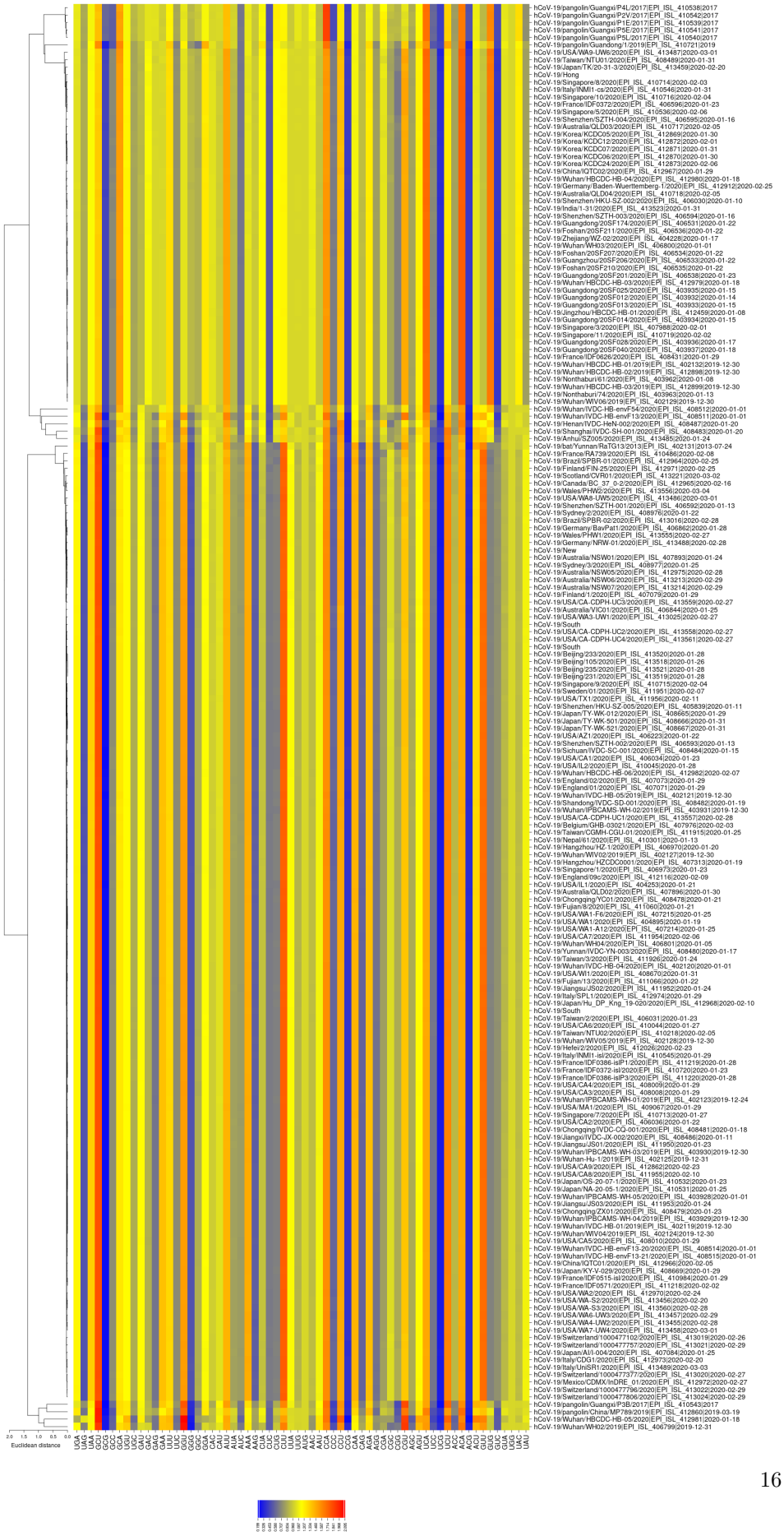

Figure 8. Heatmap of RSCU. Patterns of RSCU vectors for 306 patients affected by 2019-nCoV from different countries.

bioRxiv preprint doi: https://doi.org/10.1101/2020.03.25.006569; this version posted March 27, 2020. The copyright holder for this preprint (which was not certified by peer review) is the author/funder. All rights reserved. No reuse allowed without permission.

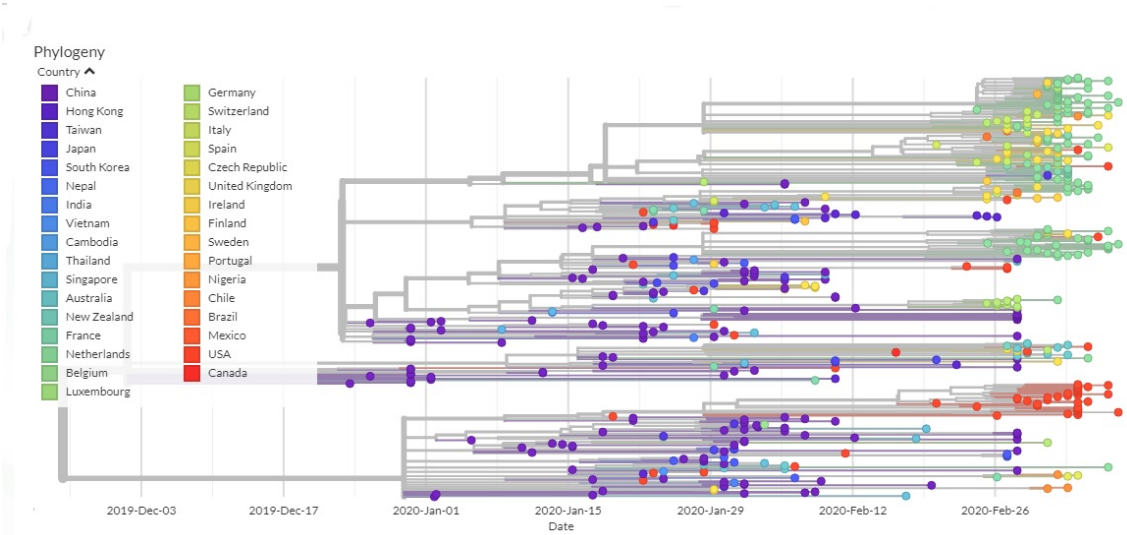

Figure 9. Phylogenetic tree from GIDAID.

7. Dilucca M, Cimini G, Giansanti A. Essentiality, conservation, evolutionary pressure and codon bias in bacterial genomes, Gene. 2018 Jul 15;663:178-188. doi: 10.1016/j.gene.2018.04.017. Epub 2018 Apr 18
8. Forcelloni, S, Giansanti A .Mutations in disordered proteins as early indicators of nucleic acid changes triggering speciation. Sci Rep 10, 4467 (2020). https://doi.org/10.1038/s41598-020-61466-5
9. Forni D, Cagliani R, Clerici M, Sironi M. Molecular Evolution of Human Coronavirus Genomes. Trends Microbiol. 2017; 25:35-48
10. Gorbalenya AE, Luis Enjuanes, JohnZiebuhr, Eric J.Snijdera. Nidovirales: Evolving the largest RNA virus genome, Volume 117, Issue 1, April 2006, Pages 17-37 https://doi.org/10.1016/j.virusres.2006.01.017
11. Grantham R, Gautier C, Gouy M, Mercier R and Pavé A. Codon catalog usage and the genome hypothesis, Nucleic Acids Research, vol. 8, no. 1, pp. r49–r62, 1980
12. Gu W., Zhou T. Analysis of synonimous codon usage in SARS Coronavirus and other viruses in the Nidovirales, Virus Res. 2004 May;101(2):155-61
13. Jenkins GM and Holmes EC. The extent of codon usage bias in human RNA viruses and its evolutionary origin, Virus Research, vol. 92, no. 1, pp. 1–7, 2003
14. Ji W, Wang W, Zhao X, Zai J, Li X. Cross-species transmission of the newly identified coronavirus 2019-nCoV. J Med Virol. 2020;92: 433–440. https://doi.org/10.1002/jmv.25682
15. Kumar S Stecher G, Li M, Knyaz C, Tamura K. MEGA X: Molecular Evolutionary Genetics Analysis across Computing Platforms.Mol Biol Evol. 2018 Jun 1;35(6):1547-1549. doi: 10.1093/molbev/msy096
16. Lia G, Wang H, Wanga S, Xinga G, Zhanga C, Zhanga W. Insights into the genetic and host adaptability of emerging porcine circovirus , VIRULENCE 2018, VOL. 9, NO. 1, 1301–1313 https://doi.org/10.1080/21505594.2018.1492863
17. Neuman BW, Kiss G, Kunding AH, Bhella D, Baksh MF, Connelly S. A structural analysis of M protein in coronavirus assembly and morphology J. Struct. Biol., 174 (2011), pp. 11-22

bioRxiv preprint doi: https://doi.org/10.1101/2020.03.25.006569; this version posted March 27, 2020. The copyright holder for this preprint (which was not certified by peer review) is the author/funder. All rights reserved. No reuse allowed without permission.

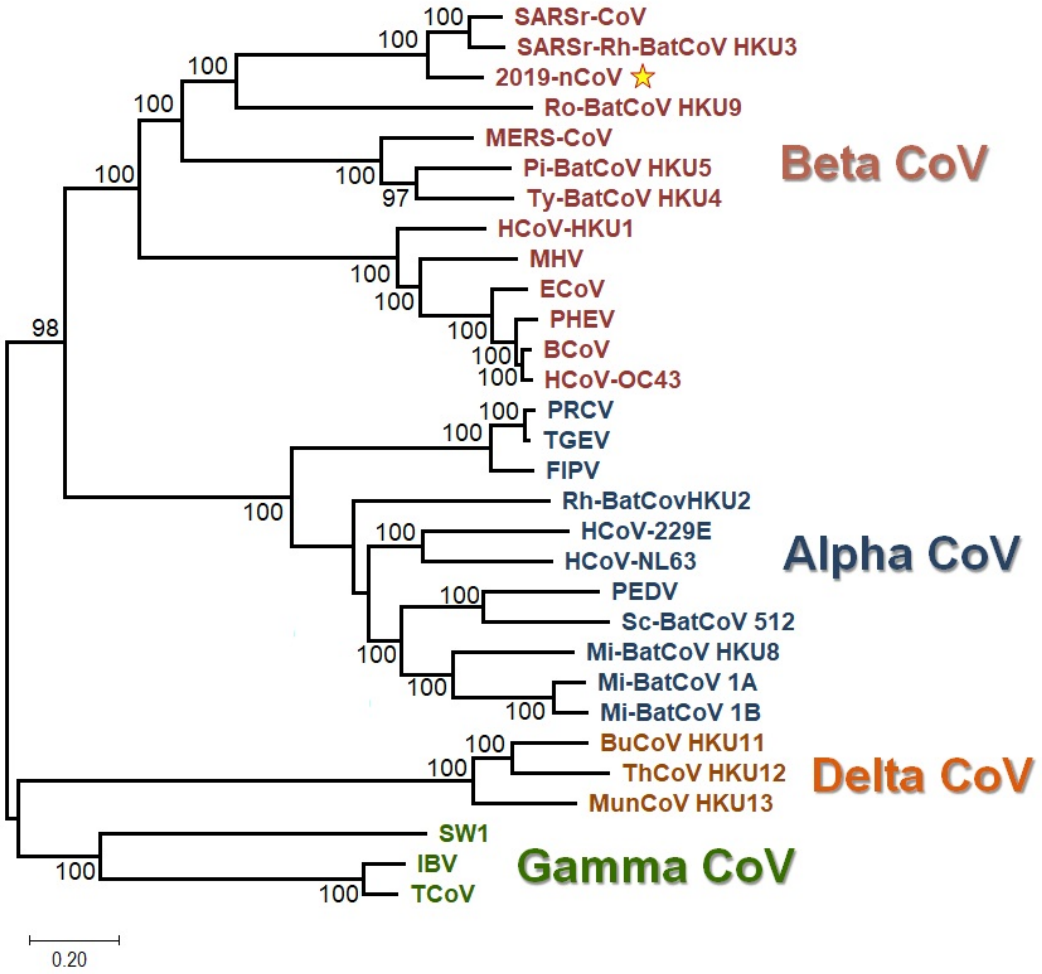

Figure 10. Unrooted ML-based tree of the 30 CoV genomic sequences. The four distinct color-coded clades correspond to the respective genera of CoVs. The 2019-nCoV sequence is indicated by a star. The branch lengths depict evolutionary distance. Bootstrap values higher than 50 are shown at the nodes. The scale bar at the lower left denotes the length of nucleotide substitutions per position.

bioRxiv preprint doi: https://doi.org/10.1101/2020.03.25.006569; this version posted March 27, 2020. The copyright holder for this preprint (which was not certified by peer review) is the author/funder. All rights reserved. No reuse allowed without permission.

18. Ruch T, Machamer C. The coronavirus E protein: assembly and beyond Viruses, 4 (2012), pp. 363-382

19. Sheihk. Analysis of preferred codon usage in the coronavirus N genes and their implications for genome evolution and vaccine design, Journal of Virological Methods 277 (2020) 113806

20. Siddell SG, Ziebuhr J, Snijder EJ. Coronaviruses, Toroviruses, and Arteriviruses. Topley and Wilson's Microbiology and Microbial Infections (2005)

21. Sievers F, Higgins DG. Clustal omega. Curr Protoc Bioinformatics. 2014 Dec 12;48:3.13.1-16. doi: 10.1002/0471250953.bi0313s48

22. Sievers F, Higgins DG. Methods Mol Biol. 2014;1079:105-16. doi: $10.1007/978-1-62703-646-7_6$ Clustal Omega, accurate alignment of very large numbers of sequences

23. Sueoka N. Directional mutation pressure and neutral molecular evolution. Proc Natl Acad Sci U S A. 1988; 85:2653-2657

24. Timani KA, Ye L, Ye L, Zhu Y, Wu Z, Gong Z. Cloning, sequencing, expression, and purification of SARS-associated coronavirus nucleocapsid protein for serodiagnosis of SARS, J Clin Virol. 2004 Aug;30(4):309-12.

25. Weinstein JN, Myers TG, O'Connor PM, Friend SH, Fornace AJ Jr, Kohn KW, Fojo T, Bates SE, Rubinstein LV, Anderson NL, Buolamwini JK, van Osdol WW, Monks AP, Scudiero DA, Sausville EA, Zaharevitz DW, Bunow B, Viswanadhan VN, Johnson GS, Wittes RE, Paull KD (1997) An information-intensive approach to the molecular pharmacology of cancer. Science 275(5298):343–9

26. Woo PC, Huang Y, Lau SK, Yuen KY. Coronavirus genomics and bioinformatics analysis. Viruses 2010 Aug;2(8):1804-20. doi: 10.3390/v2081803. Epub 2010 Aug 24. PMID: 21994708; PMCID: PMC3185738

27. Woo PC, Wong BH, Huang Y, Lau SK, Yuen KY. Cytosine deamination and selection of CpG suppressed clones are the two major independent biological forces that shape codon usage bias in coronaviruses, Virology 2007, 369, 431-442

28. Woo PC, Lau Y, Huang Y, Yuen KY. Coronavirus Diversity, Phylogeny and Interspecies Jumping. Experimental Biology and Medicine, 234(10), 1117–1127.(2009). https://doi.org/10.3181/0903-MR-94

29. Wright F. The 'effective number of codons' used in a gene, Gene. 1990 Mar 1;87(1):23-9

30. Wu A, Peng Y et al. Genome Composition and Divergence of the Novel Coronavirus (2019-nCoV) Originating in China Cell Host Microbe, Cell Host Microbe. 2020 Mar 11;27(3):325-328. doi: 10.1016/j.chom.2020.02.001. Epub 2020 Feb 7

31. Xia X. DAMBE5: a comprehensive software package for data analysis in molecular biology and evolution. Mol Biol Evol. 2013;30(7):1720-8, doi:10.1093/molbev/mst064

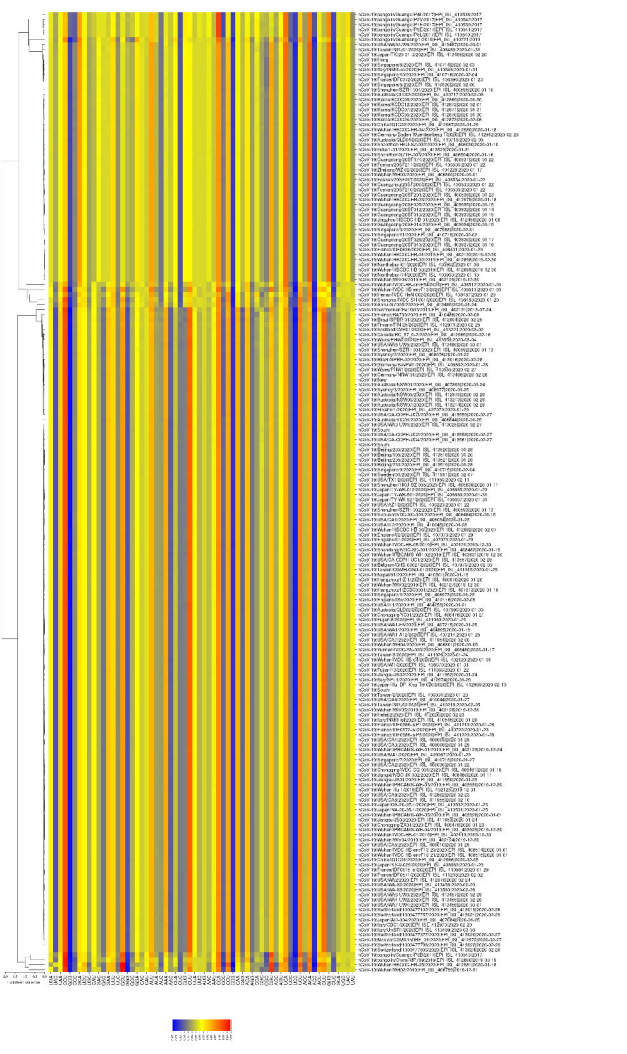

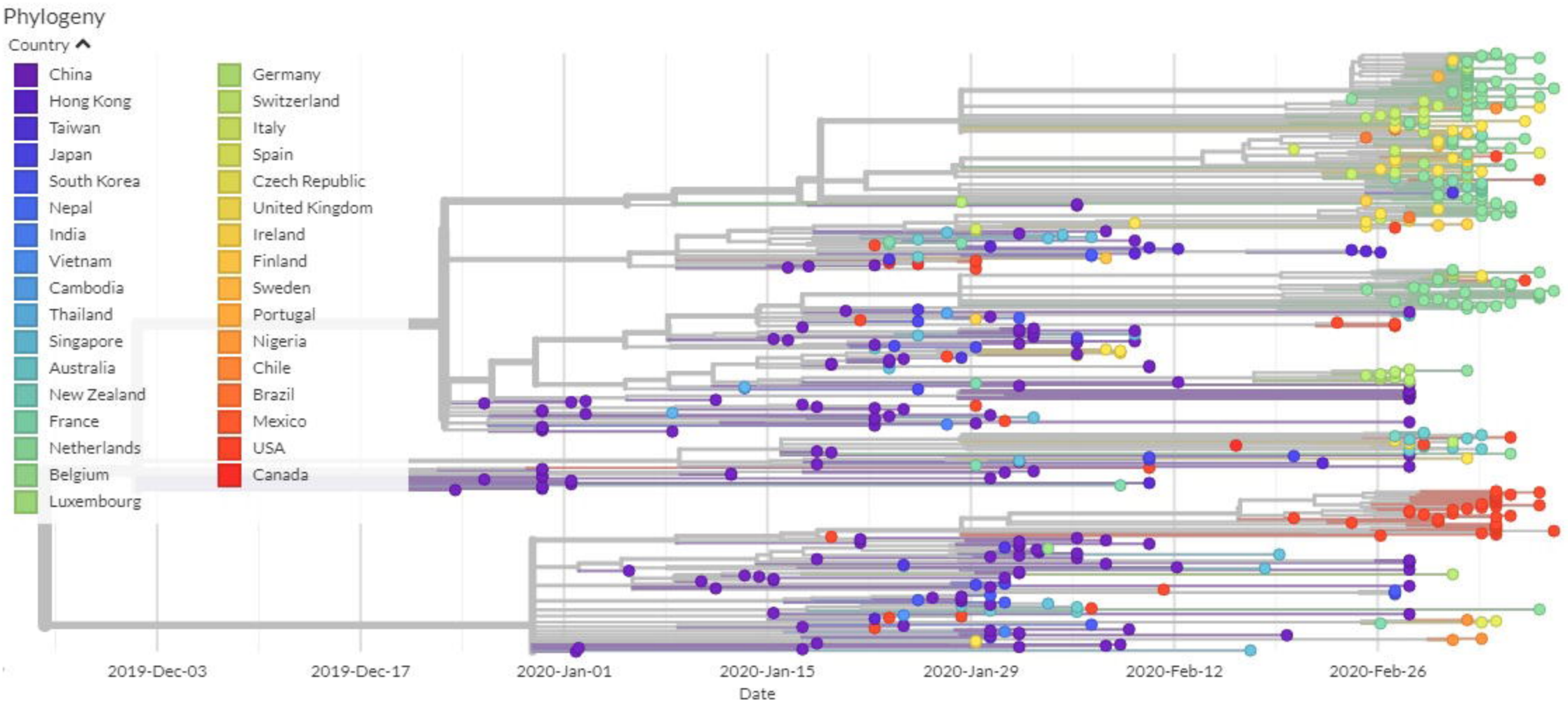
Phylogeny
Country
China
Hong Kong
Taiwan
Japan
South Korea
Nepal
India
Vietnam
Cambodia
Thailand
Singapore
Australia
New Zealand
France
Netherlands
Belgium
Luxembourg
Germany
Switzerland
Italy
Spain
Czech Republic
United Kingdom
Ireland
Finland
Sweden
Portugal
Nigeria
Chile
Brazil
Mexico
USA
Canada
2019-Dec-03
2019-Dec-17
2020-Jan-01
2020-Jan-15
2020-Jan-29
2020-Feb-12
2020-Feb-26
Date

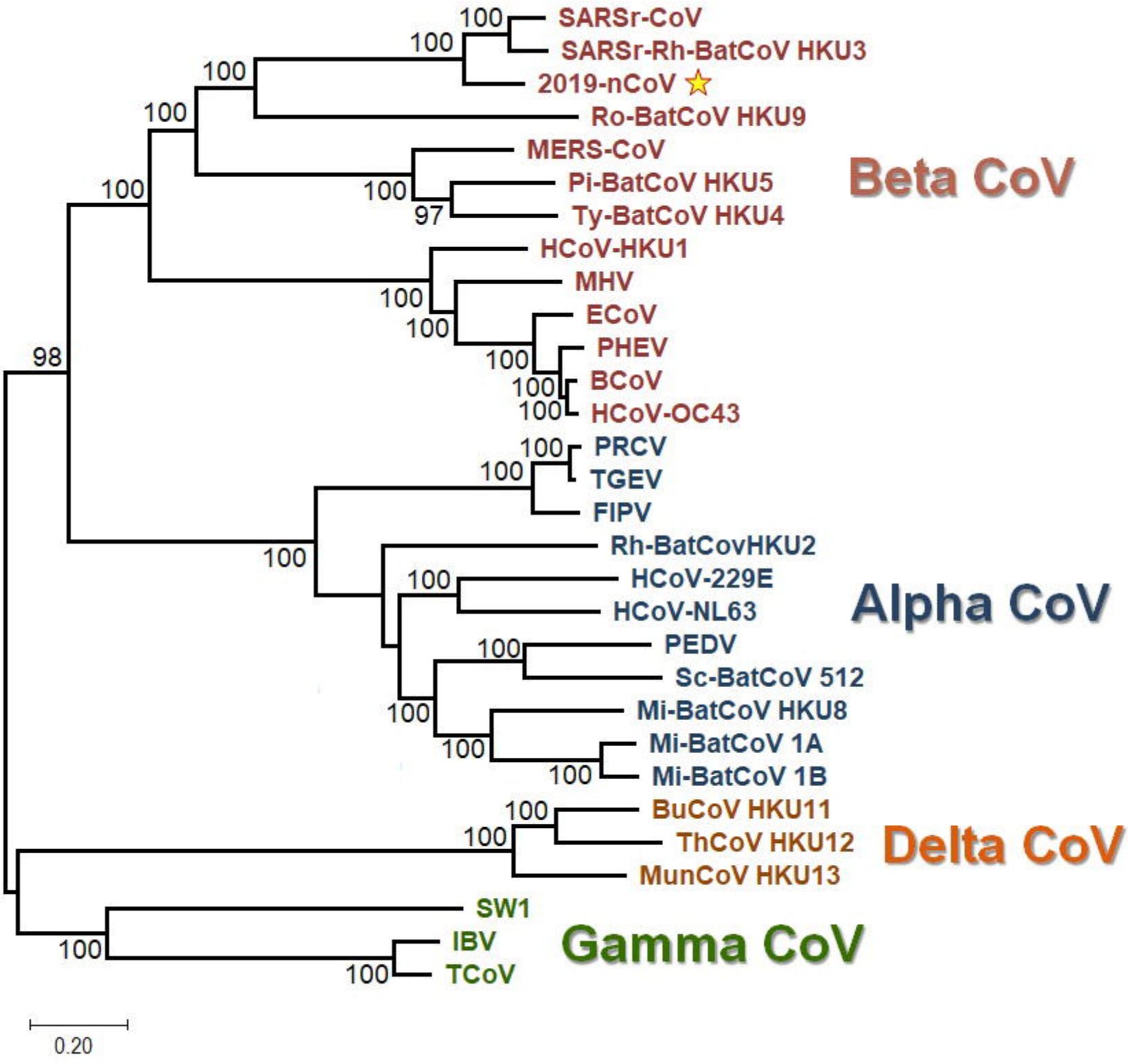
SARSr-CoV
SARSr-Rh-BatCoV HKU3
2019-nCoV
Ro-BatCoV HKU9
MERS-CoV
Pi-BatCoV HKU5
Ty-BatCoV HKU4
HCoV-HKU1
MHV
ECoV
PHEV
BCoV
HCoV-OC43
PRCV
TGEV
FIPV
Rh-BatCovHKU2
HCoV-229E
HCoV-NL63
PEDV
Sc-BatCoV 512
Mi-BatCoV HKU8
Mi-BatCoV 1A
Mi-BatCoV 1B
BuCoV HKU11
ThCoV HKU12
MunCoV HKU13
SW1
IBV
TCoV
Beta CoV
Alpha CoV
Delta CoV
Gamma CoV
0.20

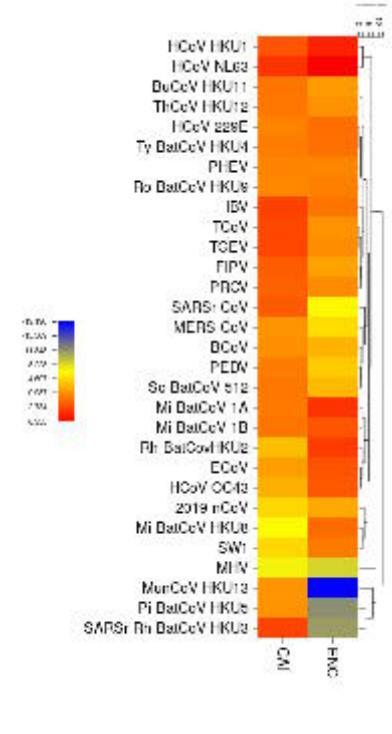
HCoV HKU1
HCoV NL63
DeCoV HKU11
ThCoV HKU12
HCoV 229E
Ty BatCoV HKU4
PHEV
Ro BatCoV HKU9
IBV
TCoV
TGEV
FIPV
PRCV
SARS-CoV
MERS-CoV
BCoV
PEDV
Sc BatCoV 512
Mi BatCoV 1A
Mi BatCoV 1B
Rh BatCoV HKU2
ECoV
HCoV OC43
2019-nCoV
Mi BatCoV HKU8
SW1
MHV
MorCoV HKU13
Pi BatCoV HKU5
SARS-Rh BatCoV HKU3
CM
FMC

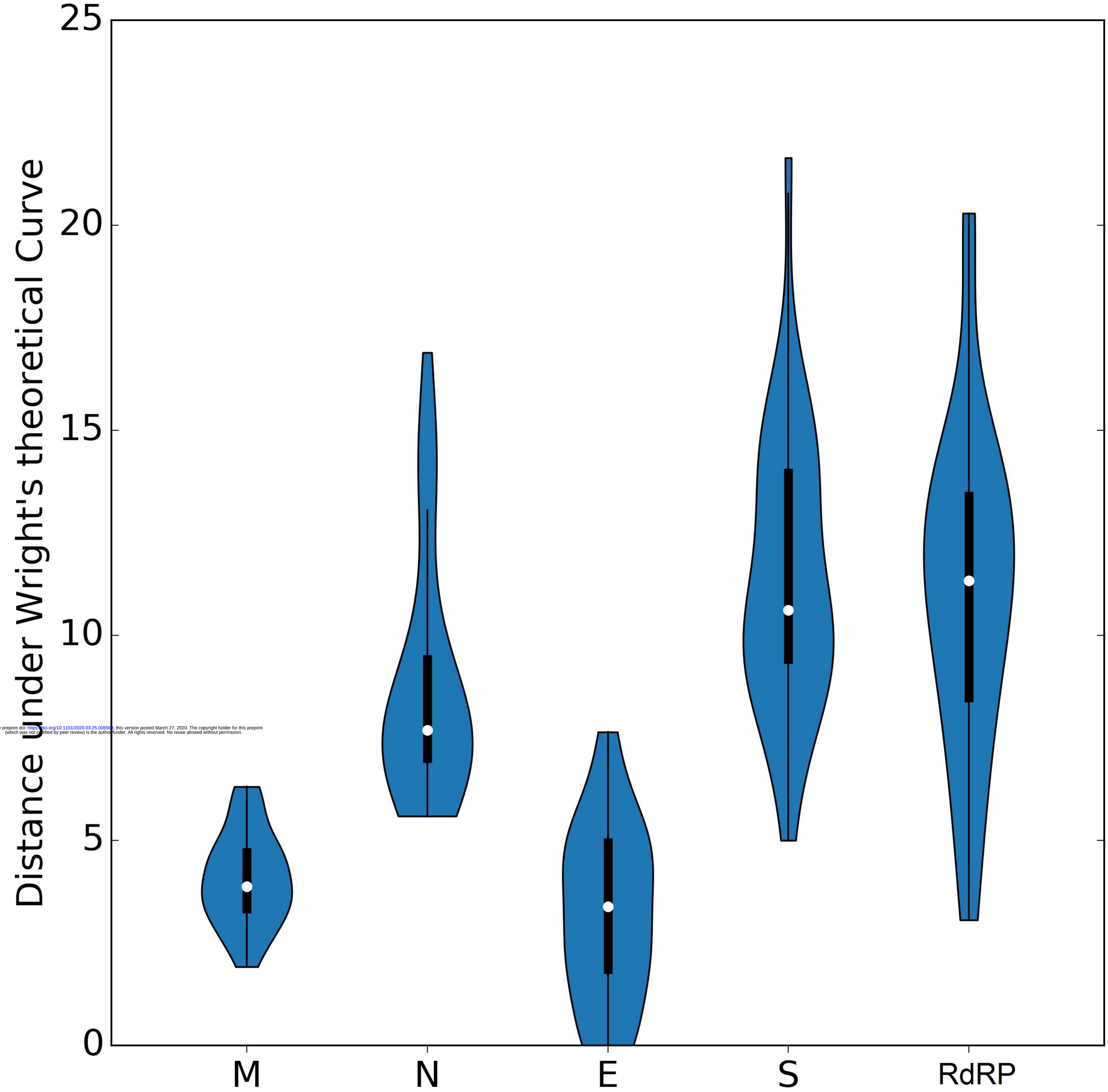

bioRxiv preprint doi: https://doi.org/10.1101/2020.03.25.006568; this version posted March 27, 2020. The copyright holder for this preprint (which was not certified by peer review) is the author/funder. All rights reserved. No reuse allowed without permission.

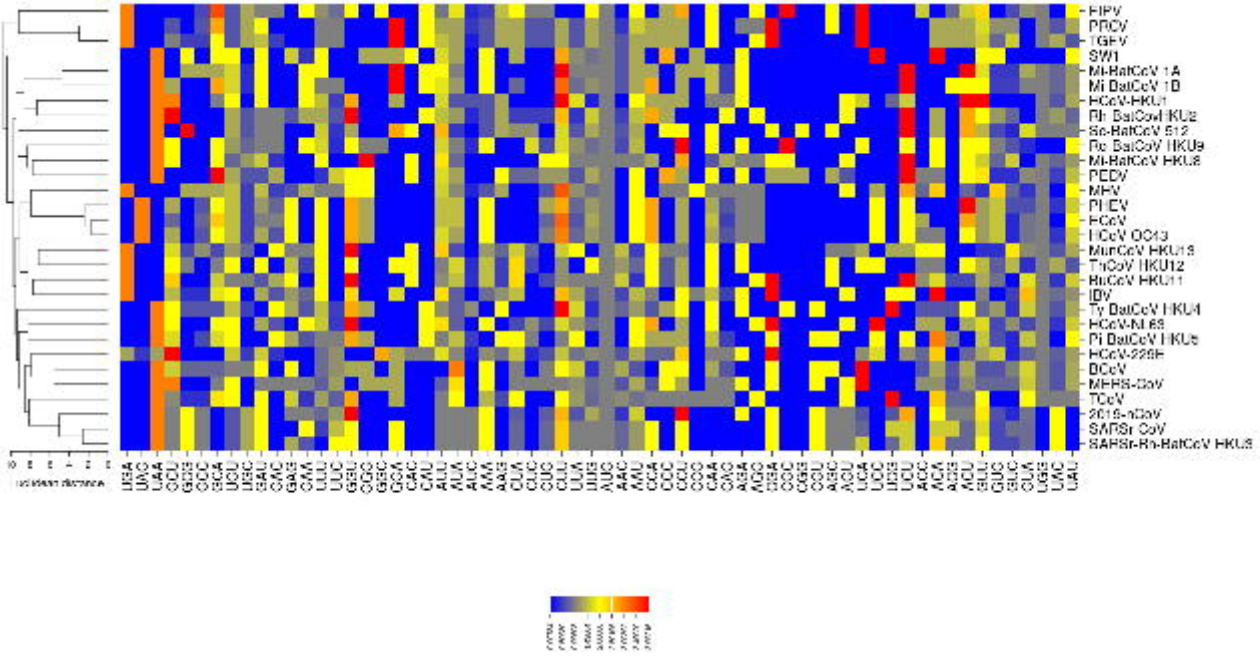
FIPV
PRCV
TGEV
SW1
Mi-BatCoV 1A
Mi BatCoV 1B
HCoV-HKU1
Rh BatCoV HKU2
Sc-BatCoV 512
Rc BatCoV HKU9
Mi-BatCoV HKU8
PEDV
MHV
PHEV
HCoV
HCoV OC43
MunCoV HKU13
ThCoV HKU12
BuCoV HKU11
IBV
Ty BatCoV HKU4
HCoV-NL63
Pi BatCoV HKU5
HCoV-229E
BCoV
MERS-CoV
TCoV
2019-nCoV
SARSr CoV
SARSr-Rh-BatCoV HKU3
ucidean distance

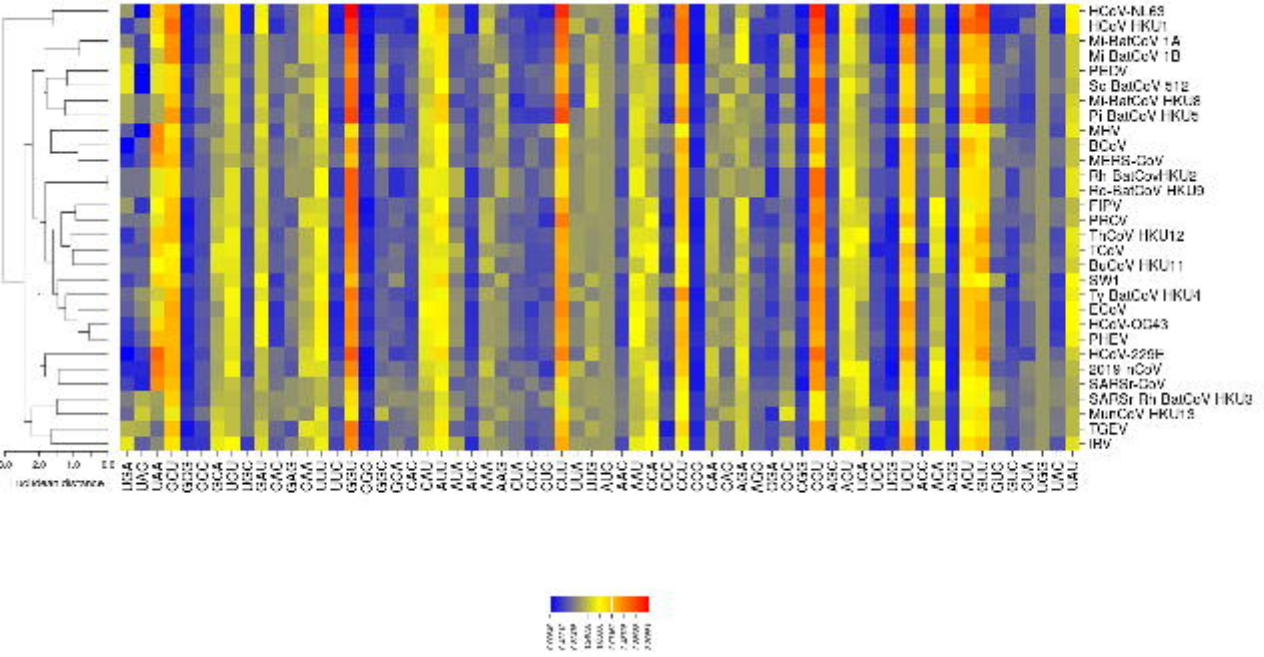
HCoV-NL63
HCoV HKU1
Mi-BatCoV 1A
Mi BatCoV 1B
PEDV
Sc BatCoV 512
Mi-BatCoV HKU8
Pi BatCoV HKU5
MHV
BCoV
MERS-CoV
Rh BatCoV HKU2
Rc-BatCoV HKU9
FIPV
PRCV
ThCoV HKU12
TCoV
BuCoV HKU11
SW1
Ty BatCoV HKU4
ECoV
HCoV-OC43
PHEV
HCoV-229E
2019 nCoV
SARSr-CoV
SARSr Rh BatCoV HKU3
MunCoV HKU13
TGEV
IBV
0.0
2.0
1.0
0.0
uclidean distance

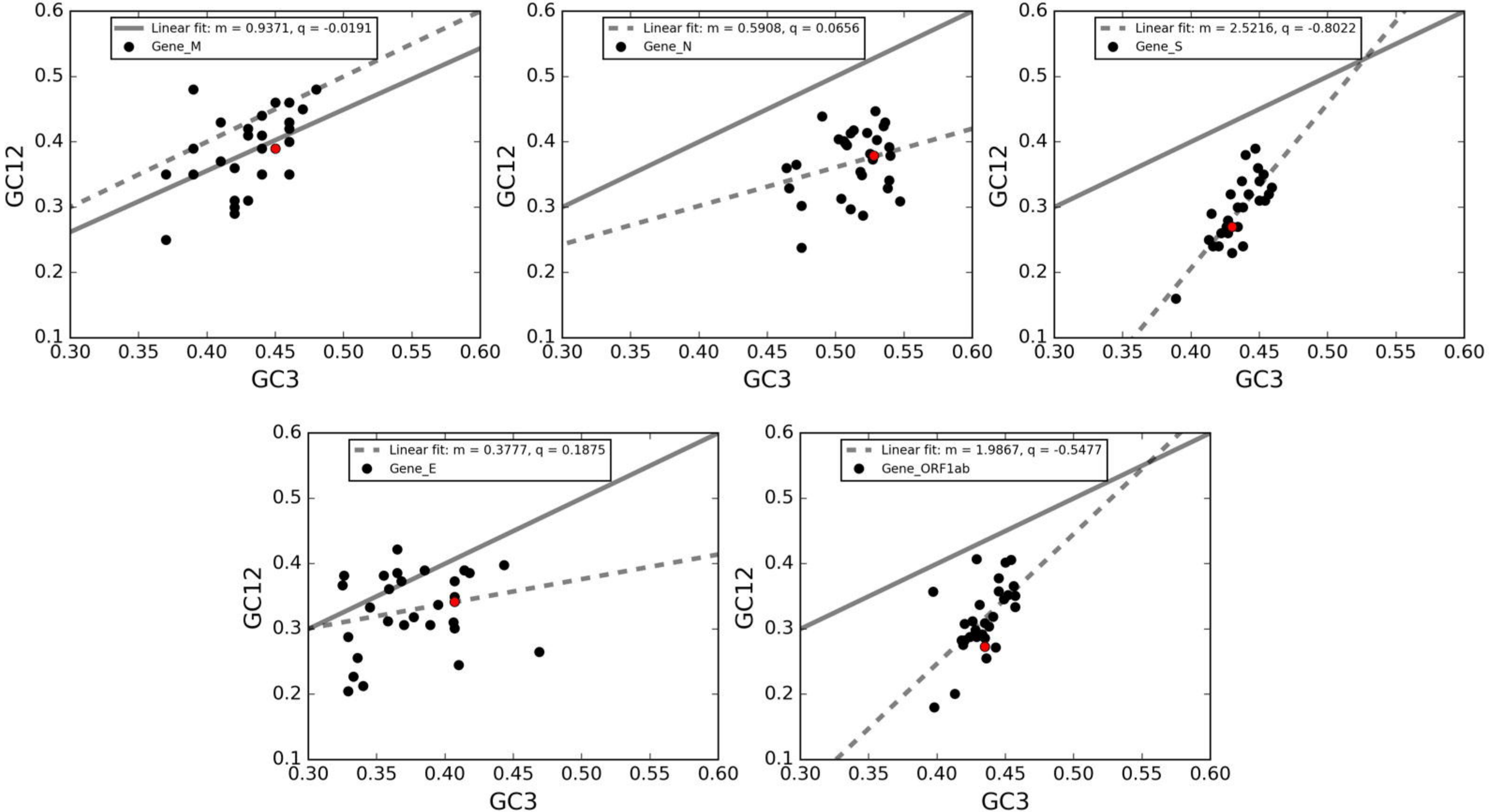
Linear fit: m = 0.9371, q = -0.0191
Gene_M
Linear fit: m = 0.5908, q = 0.0656
Gene_N
Linear fit: m = 2.5216, q = -0.8022
Gene_S
Linear fit: m = 0.3777, q = 0.1875
Gene_E
Linear fit: m = 1.9867, q = -0.5477
Gene_ORF1ab
GC12
GC3
0.1
0.2
0.3
0.4
0.5
0.6
0.30
0.35
0.40
0.45
0.50
0.55
0.60

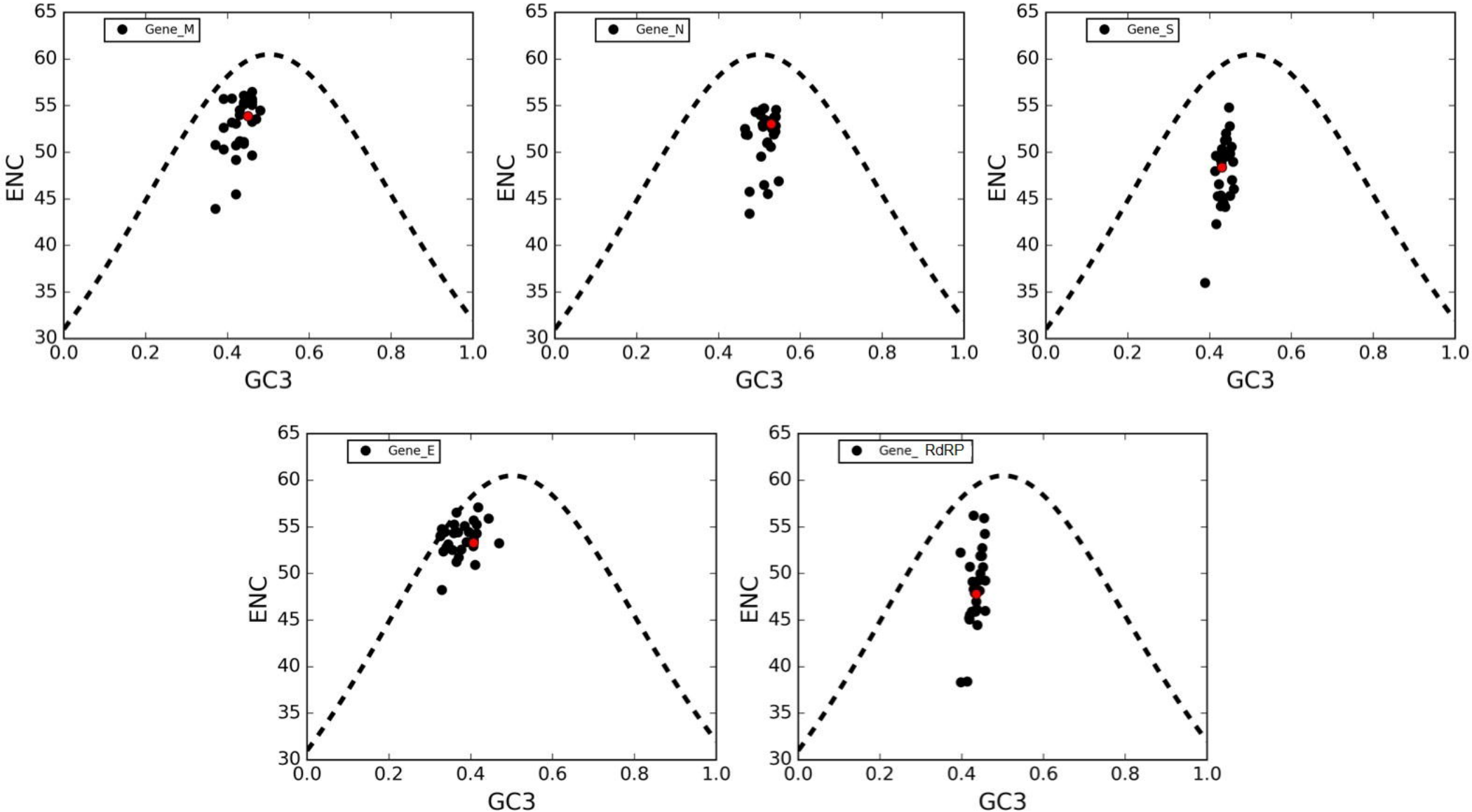
Gene_M
Gene_N
Gene_S
Gene_E
Gene_ RdRP
ENC
GC3
65
60
55
50
45
40
35
30
0.0
0.2
0.4
0.6
0.8
1.0

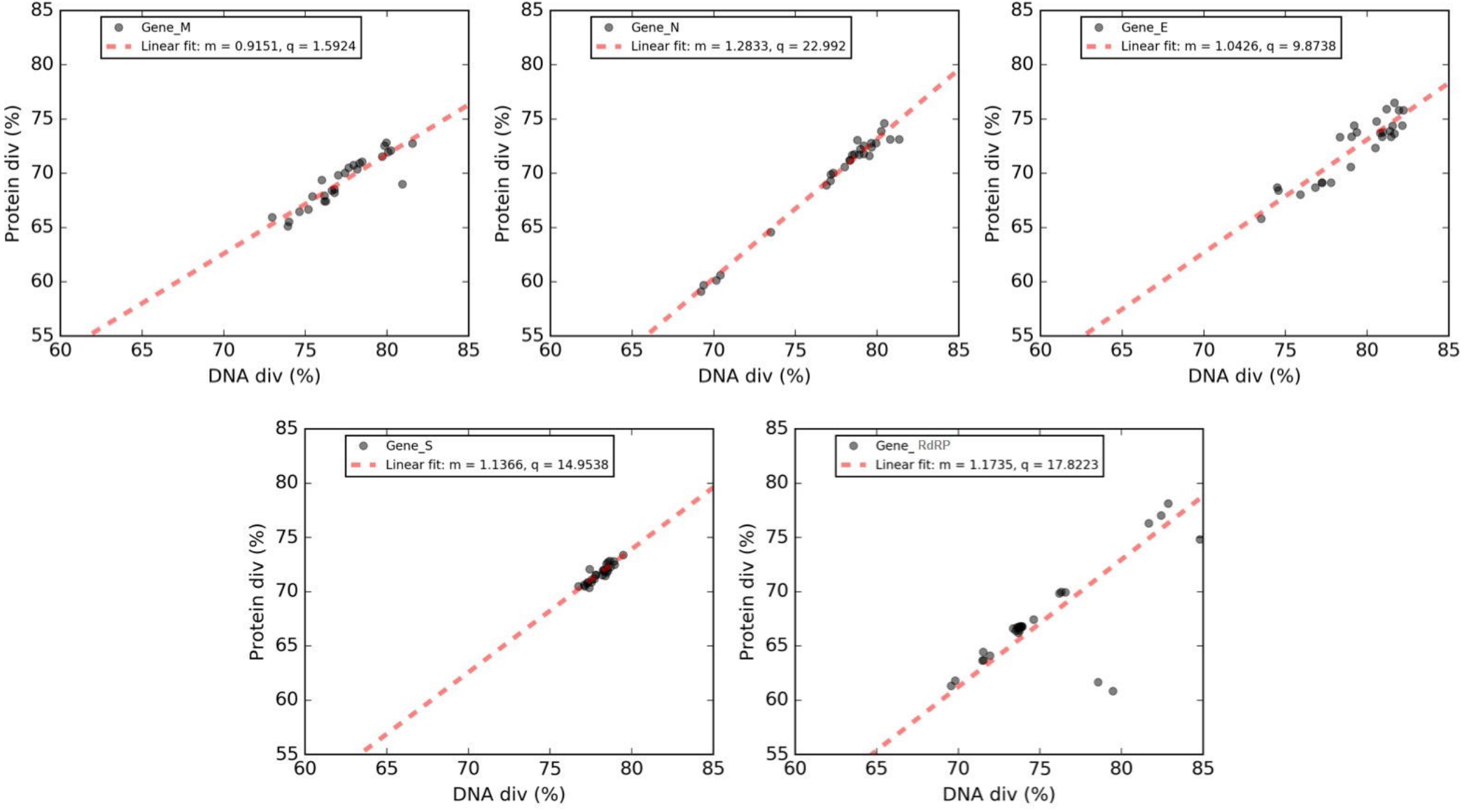
Gene_M
Linear fit: m = 0.9151, q = 1.5924
Gene_N
Linear fit: m = 1.2833, q = 22.992
Gene_E
Linear fit: m = 1.0426, q = 9.8738
Gene_S
Linear fit: m = 1.1366, q = 14.9538
Gene_ RdRP
Linear fit: m = 1.1735, q = 17.8223
Protein div (%)
DNA div (%)
55
60
65
70
75
80
85

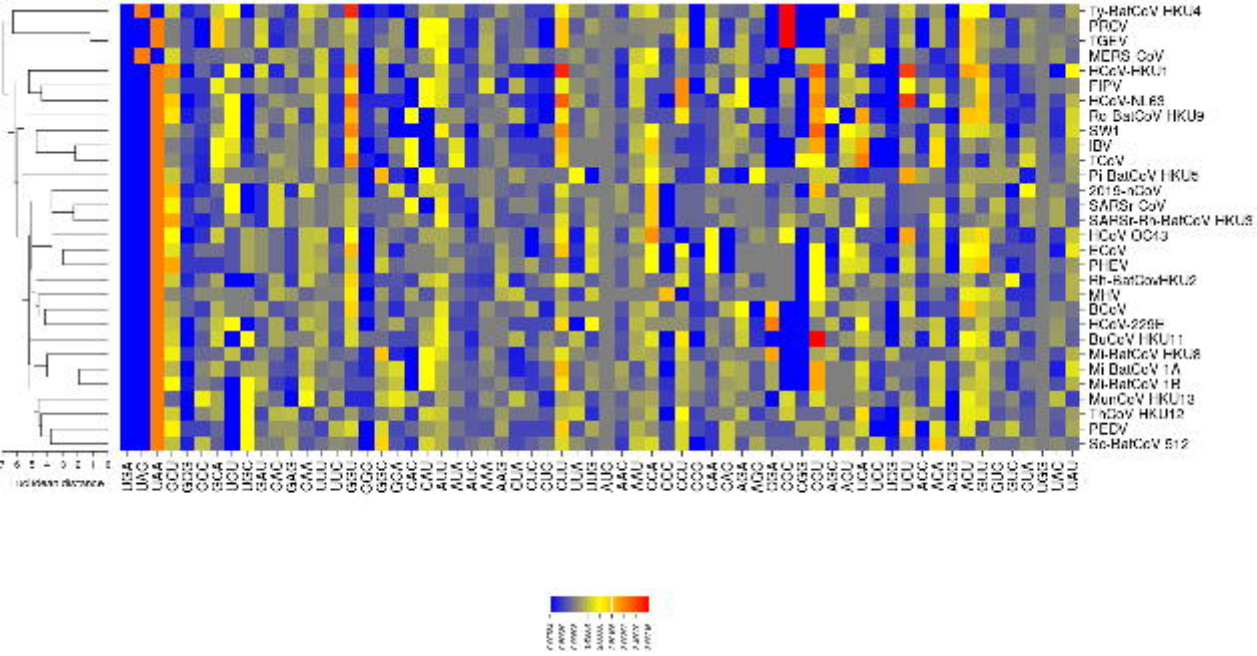

Ty-BatCoV HKU4
PRCV
TGEV
MERS CoV
HCoV-HKU1
FIPV
HCoV-NL63
Rc BatCoV HKU9
SW1
IBV
TCoV
Pi BatCoV HKU5
2019-nCoV
SARSr CoV
SARSr-Rh-BatCoV HKU3
HCoV OC43
HCoV
PHEV
Rh-BatCovHKU2
MHV
BCoV
HCoV-229E
BuCoV HKU11
Mi-BatCoV HKU8
Mi BatCoV 1A
Mi-BatCoV 1B
MunCoV HKU13
ThCoV HKU12
PEDV
Sc-BatCoV 512

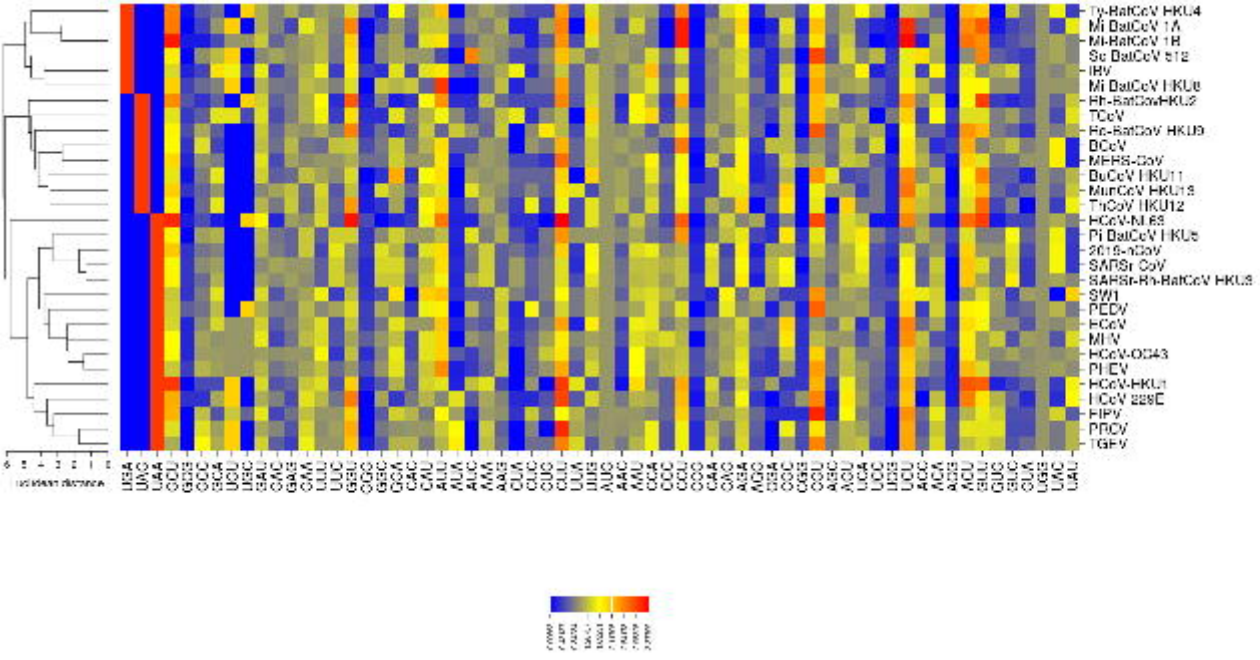
Ty-BatCoV HKU4
Mi BatCoV 1A
Mi-BatCoV 1B
Sc BatCoV 512
IBV
Mi BatCoV HKU8
Rh-BatCoVHKU2
TCoV
Rc-BatCoV HKU9
BCoV
MERS-CoV
BuCoV HKU11
MunCoV HKU13
ThCoV HKU12
HCoV-NL63
Pi BatCoV HKU5
2019-nCoV
SARSr CoV
SARSr-Rh-BatCoV HKU3
SW1
PEDV
HCoV
MHV
HCoV-OC43
PHEV
HCoV-HKU1
HCoV 229E
FIPV
PRCV
TGEV
UGA UAC UAA CCU GGG CCC GCA UCU UGC GAU CAC GAG CAA UUU UUC GGU GGC GCA CAC CAU AUU AUA AUC AAA AAG CUA CUC CUG CUU UUA UUG AUG AAC AAU CCA CCC CCU CCG CAA CAG AGA AGG GGA CCC CGG CCU AGC ACU UCA UCC UGG UCU ACC ACA AGG ACU GUU GUC GUC CUA UGG UAC UAU
0 1 2 3 4 5 6
radiation distance

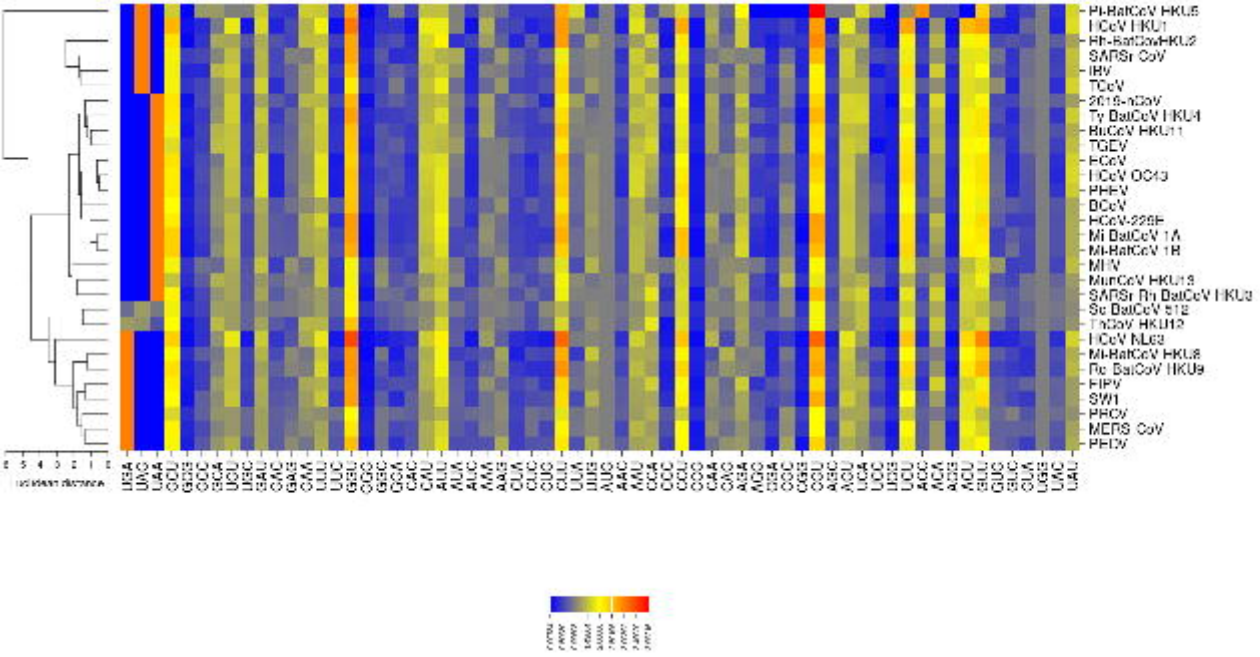
Pi-BatCoV HKU5
HCoV HKU1
Rh-BatCoVHKU2
SARSr CoV
IBV
TCoV
2019-nCoV
Ty BatCoV HKU4
BuCoV HKU11
TGEV
FCoV
HCoV OC43
PHEV
BCoV
HCoV-229E
Mi BatCoV 1A
Mi-BatCoV 1B
MHV
MunCoV HKU13
SARSr Rh BatCoV HKU3
Sc BatCoV 512
ThCoV HKU12
HCoV NL63
Mi-BatCoV HKU8
Re BatCoV HKU9
FIPV
SW1
PRCV
MERS CoV
PEDV
UGA UAG UAA CCU GGG CCC GCA UCU UGC GAU CAC GAG CAA UUU UUC GGU GGC GGC CAC CAU AUU AUA AUC AAA AAG CUA CUC CUG CUU UUA UUG AUG AAC AAU CCA CCC CCU CCG CAA CAG AGA AGG GGA CGC CGG CGU AGC AGU UCA UCC UGG UCU ACC ACA AGG ACU GUU GUC GUC CUA UGG UAC UAU
0 5 4 3 2 1 0
radian distance

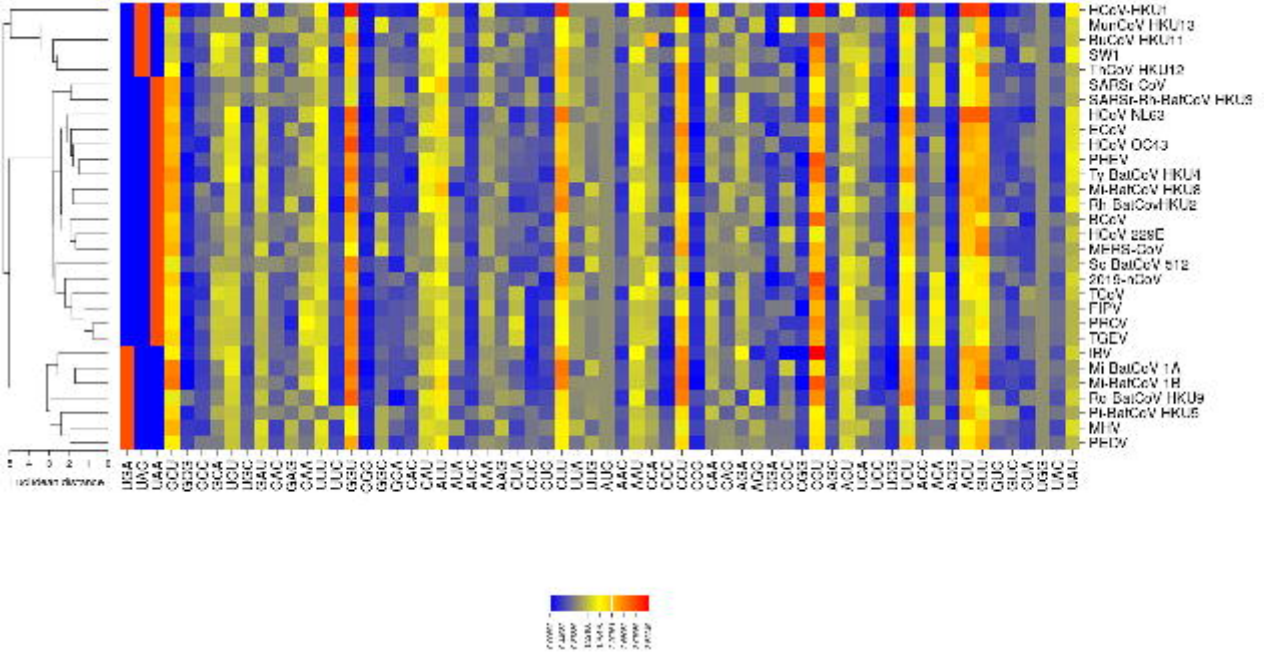
HCoV-HKU1
MunCoV HKU13
RuCoV HKU11
SW1
ThCoV HKU12
SARSr CoV
SARSr-Rh-BatCoV HKU3
HCoV NL63
HCoV
HCoV OC43
PHEV
Ty BatCoV HKU4
Mi-BatCoV HKU8
Rh BatCoV HKU2
BCoV
HCoV 229E
MERS-CoV
Sc BatCoV 512
2019-nCoV
TCoV
FIPV
PRCV
TGEV
IBV
Mi BatCoV 1A
Mi-BatCoV 1B
Rc BatCoV HKU9
Pi-BatCoV HKU5
MHV
PEDV
UGA UAC UAA CCU GCG CCC GCA UCU UGC GAU CAC GAG CAA UUU UUC GGU GGC GGC CAC CAU ALU AUA AUC AAA AAG CUA CUC CUC CUU UUA UUG AUC AAC AAU CCA CCC CCU CCC CAA CAC AGA AGC GGA CGC CGG CGU AGC AGU UCA UCC UCG UCU ACC ACA ACG ACU GUU GUC GUC CUA UGG UAC UAU